



A novel fractional discrete grey model with variable weight buffer operator and its applications in renewable energy prediction

Yong Wang¹ · Pei Chi¹ · Rui Nie¹ · Xin Ma² · Wenqing Wu² · Binghong Guo¹

Accepted: 30 March 2023 / Published online: 21 April 2023

© The Author(s), under exclusive licence to Springer-Verlag GmbH Germany, part of Springer Nature 2023

Abstract

With the continuous depletion of global fossil energy, optimizing the energy structure has become the focus of attention of all countries. With the support of policy and finance, renewable energy occupies an important position in the energy structure of the USA. Being able to predict the trend of renewable energy consumption in advance plays a vital role in economic development and policymaking. Aiming at the small and changeable annual data of renewable energy consumption in the USA, a fractional delay discrete model of variable weight buffer operator based on grey wolf optimizer is proposed in this paper. Firstly, the variable weight buffer operator method is used to preprocess the data, and then, a new model is constructed by using the discrete modeling method and the concept of fractional delay term. The parameter estimation and time response formula of the new model are deduced, and it is proved that the new model combined with the variable weight buffer operator satisfies the new information priority principle of the final modeling data. The grey wolf optimizer is used to optimize the order of the new model and the weight of the variable weight buffer operator. Based on the renewable energy consumption data of solar energy, total biomass energy and wind energy in the field of renewable energy, the grey prediction model is established. The results show that the model has better prediction accuracy, adaptability and stability than the other five models mentioned in this paper. According to the forecast results, the consumption of solar and wind energy in the USA will increase incrementally in the coming years, while the consumption of biomass will decrease year by year.

Keywords Fractional discrete grey model · Variable weight buffer operator · New information priority · Grey wolf optimizer · Renewable energy prediction

1 Introduction

1.1 Background

With the development of science and technology, the demand and consumption of energy in the world are increasing. At the same time, people pay more and more attention to environmental protection. Therefore, the popular vocabulary of renewable energy has attracted a lot of attention (Rehbein et al. 2020; Sharif et al. 2020; Wu et al.

2019a), and the statistics and prediction of renewable energy consumption have become particularly important. To address different types of data samples, a large number of predictive models have been generated. For the prediction problem of “large sample, more data”, the method of probability and mathematical statistics can be used to solve it. Mehedintu et al. (2018) made statistics and Analysis on the economic indicators of the 28 EU countries, and estimated the consumption of renewable energy by using five regression models, and finally obtained the forecast results of 2020. Ma et al. (2018) proposed a machine learning prediction algorithm without a large number of independent variables and assumptions, and predicted the biomass and hydropower consumption in the USA. Huang et al. (2020) used the improved state transition algorithm to optimize the parameters of the Gaussian process regression method, proposed a new model, and predicted the total

✉ Yong Wang
ywangsc@qq.com

¹ School of Sciences, Southwest Petroleum University, Chengdu 610500, Sichuan, China

² School of Mathematics and Physics, Southwest University of Science and Technology, Mianyang 621010, Sichuan, China

consumption of renewable energy and the consumption of each renewable energy in China. Brodny et al. (2020) uses artificial neural network analysis to cover eight main sources of renewable energy production in Poland and forecast the sources of renewable energy production in 2025. Khan et al. (2020) combined multi-layer perceptron, support vector back and CatBoost to propose a new hybrid method for power prediction based on machine learning. By combining the idea of the random effect regression model, piecewise regression model and minimum pruning double estimation, Zhou et al. (2022) proposed a mixed effect piecewise regression model and a new robust estimation to predict the baseline power consumption in Southern California. Khan et al. (2022) combines convolutional neural network with echo state network to predict renewable energy generation and consumption. Kilic et al. (2022) used the artificial neural network method to predict the total wind and solar power generation of G8 member Germany and European countries. These methods have strict requirements on the size of the data set. However, in the early stage of industry development, the data samples obtained are less and the amount of information is relatively poor, and the probability and mathematical statistics methods for such data samples often cannot be accurately analysed.

1.2 Literature review

In order to process the time series of “small sample” and “poor data”, the Grey system theory was first put forward by Deng (1982). After more than 30 years of development, it has been widely used in energy consumption, industrial production, environment, social development decision-making, economic forecasting and other fields (Wu et al. 2020a, 2019b; Wang et al. 2023a, 2022a). Wu et al. (2018a) optimized the GM (1,n) model with convolution solution by changing the order of fractional order accumulation, combined with grey correlation analysis, and a multivariable prediction model is proposed to predict the power consumption in Shandong Province of China. Liu et al. (2020) proposed a new adjacent non-homogeneous grey model to predict renewable energy consumption in Europe. Wu et al. (2018b) proposed a new fractional grey model and applied it to the prediction of China’s nuclear energy consumption. Ma et al. (2019a) combined Bernoulli equation and GM(1,n) model with convolution solution to establish a nonlinear grey Bernoulli multivariate model and predict China’s tourism income. Based on Grunwald–Letnikov fractional calculus, Wang et al. (2022b) proposed an adaptive fractional order multivariable grey model based

on a new sequence, and predicted the total per capita energy consumption, energy conversion efficiency and total renewable energy in China. He et al. (2022) established a new discrete grey prediction model of structural adaptive new information priority, and the disturbance analysis showed that the model was suitable for small sample modeling. Zeng et al. (2020a) used a new structural grey Verhulst model to predict tight gas production in China. Wang et al. (2022c) proposed a new fractional order structure adaptive grey Chebyshev polynomial Bernoulli model and verified the model with four actual cases of renewable energy production and consumption in China. Wu et al. (2020b) used the grey Riccati model to study the consumption of oil and nuclear energy in China. Wang et al. (2022d) put forward a new grey model to forecast China’s crude oil production data. Zeng et al. (2020b), considering the influence of extreme values of independent variables, proposed a multivariable grey prediction model based on smooth generation and predicted China’s grain production. Wang et al. (2022e) proposed a structural adaptive grey model FCSAGM (p, 1) with Caputo fractional derivative and a new Caputo fractional cumulative generation operator to predict China’s energy data. Wu et al. (2020c) used the new Grey Bernoulli model to study the consumption of natural gas in the USA, Germany, the United Kingdom, China and Japan. Wang et al. (2022f) introduced the time delay term and Bernoulli equation, proposed a new fractional order time delay grey Bernoulli model, and predicted the development trend of renewable energy, crude oil and fossil fuels. In order to reduce the interference of data collection and statistics, and to explore the internal relationship of data, Liu first proposed the concept of buffer operator in 1990 (Yamaguchi et al. 2007). Subsequently, a large number of scholars have innovated and optimized it on the basis of it, and proposed the average buffer operator (Zeng et al. 2020c), the weighted average buffer operator (Xie and Liu 2003), the variable weight buffer operator (Wang et al. 2009), the multivariable buffer operator (Wu et al. 2016). Therefore, for a small sample of annual data on renewable energy consumption in the USA, the grey prediction model shows unique advantages.

Because the univariate grey forecasting model only needs to use a single time series to model and predict the time series, the GM(1,1) model has the advantages of simple operation and convenient operation and has been extensively studied (Ma et al. 2019b). In order to enhance the tendency catching ability of GM(1,1) model, Xie and Liu proposed a more accurate discrete model DGM(1,1) by using the discrete modeling method (Xie and Liu 2009). In

practical application, because of the complexity of time series, the integer-order model shows its own limitations. In order to improve the accuracy of integer order model and enhance the applicability of the single variable model, many scholars have established fractional order modeling technology (Ma et al. 2020) and put forward a large number of fractional grey models (Ma et al. 2019c; Wu et al. 2019c). Wu et al. (2013) defined the fractional order accumulation theory by using binomials and established the FGM(1,1) model on this basis. Meng et al. (2020) established the FDGM(1,1) model by using the unified fractional grey accumulation generating operator. In Zeng et al. (2020d) by introducing the non-homogeneous exponential function into the traditional Verhulst model, the structural defects of the traditional Verhulst model were improved, and the N_Verhulst model with the stronger modeling ability was proposed. Most models do not consider the influence of time delay in the process of modeling. Zhang et al. (2015) introduced the time delay term into the grey model and proposed a multivariate time delay grey model. Yu et al. (2021a) considered the time delay power effect with high flexibility and established a grey model of time delay power-driven. Ma et al. (2019d) revealed the essence of fractional order time delayed and proposed a fractional time delayed grey model. Wang et al. (2021) combined the Hausdorff fractional accumulation operator and Grunwald–Letnikov fractional derivative to improve the GM(1,n) model of kernel regularization nonlinear with convolution solution, and proposed a Hausdorff fractional-order nonlinear grey prediction model. Lu et al. (2021b) proposed a hybrid method combining elastic networks and multi-objective optimization to optimize nonlinear grey Bernoulli multivariate models. Wu et al. (2021) used Simpson numerical integration formula to construct the background value and proposed a new discrete grey prediction model. Wang et al. (2022g) defined a new fractional order self-adaptive accumulation sequence, introduced the time power term and discrete modeling techniques, and proposed a self-adaptive reverse accumulation discrete grey model with time power term. Wang et al. (2023b) proposed a self-adaptive fractional grey Euler model with dynamic accumulation order and used the model to forecast energy production of China. Yao et al. (2022) studied the representation of bifinite domains by rough approximable concepts. Yan et al. (2022) revealed a broadband vibration energy harvester based on nonlinear magnetic force and rotary pendulums. Feng et al. (2020) considered the almost periodic solutions for certain differential equations with piecewise constant arguments. Dai et al. (2014) introduced

a multi-parameter magnetoelectric response modeling of magnetostrictive laminate. Wang et al. (2017, 2018a, 2019, 2020a) studied the optimizing injection process of water-alternate-gas using different produced gas. Wang et al. (2020b, 2020c) (Wang and Yi 2018) proposed the dynamic analysis of oil–water two-phase flow for a multiple-fractured horizontal well with multiple finite-conductivity fractures in triple media carbonate reservoir. Wang et al. (2017, 2018b, 2018c) considered the nonlinear oil–water two-phase flow behaviour for a horizontal well in triple media carbonate reservoir.

1.3 Contribution and motivation

However, some models do not consider the interference of the data itself, which leads to the accuracy of the grey prediction model is not ideal. At the same time, the integer modeling technology cannot fine-tune the model, which limits the flexibility and application scope of the model. In this paper, the operation of the variable weight buffer operator is used to reduce the interference of system data. Combined with the concept of fractional delay, the discrete modeling method is used, and the Grey Wolf Optimizer (GWO) (Mirjalili 2015) is used to optimize the parameters. A novel fractional delay discrete model with variable weight buffer operator is established. For this, we derive the parameter estimation and time response formula of the new model. Finally, we established a prediction model for the US solar, biomass and wind energy data sets. Compared with other models, the main innovations and contributions of this paper are as follows:

- (1) This paper introduces the concept of variable weight buffer operator and proves that the combination of the new model and variable weight buffer operator satisfies the new information first principle of the latest modeling data;
- (2) In this paper, a fractional delay discrete model with variable weight buffer operator is proposed. Its prediction accuracy is better than the other five models, and FTDDGM(1,1) has the smallest range of change and better stability than the other five models;
- (3) In this paper, the Grey Wolf optimizer is used to optimize the two parameters of FTDDGM(1,1) with variable weight buffer operator;
- (4) This paper can reasonably predict the renewable energy consumption in the USA and can provide

reference for policy formulation, government expenditure arrangement and project planning.

The rest of this paper is arranged as follows: In Sect. 2, the fractional order discrete time delay model (FTDDGM(1,1)) is proposed, and the parameter estimation equation and time response formula of the new model are derived. It is proved that the new model satisfies the new information priority principle of the last modeling data. In Sect. 3, the Grey Wolf Optimizer, the two-parameter optimization steps and the modeling steps of the new model are introduced. In Sect. 4, the new model is verified in three actual cases of renewable energy consumption in the USA, and the conclusion is drawn in Sect. 5.

2 Fractional time delay discrete model with variable weight buffer operator

This section briefly introduces the definition of variable weight buffer operator and fractional order accumulation. A novel fractional time delay discrete grey prediction model is proposed.

2.1 Modeling steps of the DGM (1,1) model

Definition 1 Assuming that the original non-negative sequence is $X^{(0)} = \{x^{(0)}(1), x^{(0)}(2), \dots, x^{(0)}(n)\}$, its first-order cumulative generation sequence is $X^{(1)} = \{x^{(1)}(1), x^{(1)}(2), \dots, x^{(1)}(n)\}$, where.

$$x^{(1)}(k) = \sum_{i=1}^k x^{(0)}(i), \quad k = 1, 2, \dots, n. \tag{1}$$

Then, the discrete equation is

$$x^{(1)}(k + 1) = \beta_1 x^{(1)}(k) + \beta_2. \tag{2}$$

It is called DGM (1,1) model. Its parameters are determined as

$$\hat{\beta} = (\beta_1, \beta_2)^T = (B^T B)^{-1} B^T Y. \tag{3}$$

where

$$B = \begin{bmatrix} x^{(1)}(1) & 1 \\ x^{(1)}(2) & 1 \\ \vdots & \vdots \\ x^{(1)}(n-1) & 1 \end{bmatrix}, \quad Y = \begin{bmatrix} x^{(1)}(2) \\ x^{(1)}(3) \\ \vdots \\ x^{(1)}(n) \end{bmatrix}.$$

The time response formula of DGM (1,1) model is.

$$x^{(1)}(k + 1) = \beta_1^k \left(x^{(0)}(1) - \frac{\beta_2}{1 - \beta_1} \right) + \frac{\beta_2}{1 - \beta_1}, \quad k = 1, 2, \dots, n \tag{4}$$

The DGM (1,1) model is the first discrete grey model, which can perfectly fit a non-negative series of pure indices compared to the continuous grey model. Many discrete grey models are built on the basis of the DGM(1,1) model. The model built in this paper is also based on DGM(1,1).

2.2 The operation of variable weight buffer operator and fractional order accumulation

Definition 2 Mao et al. (2016). Assume that the non-negative sequence $X^{(0)} = \{x^{(0)}(1), x^{(0)}(2), \dots, x^{(0)}(n)\}$, its variable weight buffer sequence is $X^{(0)}D = \{x^{(0)}(1)d, x^{(0)}(2)d, \dots, x^{(0)}(n)d\}$ where

$$x^{(0)}(k)d = \lambda x^{(0)}(n) + (1 - \lambda)x^{(0)}(k), \quad 0 < \lambda < 1, \quad k = 1, 2, \dots, n \tag{5}$$

Therefore, D is called a variable weight buffer operator.

Compared with the original sequence, the variable-weighted buffer sequence has a higher priority of new information due to the inclusion of the same proportion of the latest element items in each element, which further increases the importance of new information in the model.

Definition 3 Mao et al. (2016). Let the sequence $X^{(0)} = \{x^{(0)}(1), x^{(0)}(2), \dots, x^{(0)}(n)\}$, if $X^{(r)}$ is called the fractional cumulative sequence (r -FAO) of $X^{(0)}$, then $X^{(r)} = \{x^{(r)}(1), x^{(r)}(2), \dots, x^{(r)}(n)\}$, $r \in R^+$ where

$$x^{(r)}(k) = \sum_{i=1}^k \frac{\Gamma(k+r-i)}{\Gamma(k-i+1)\Gamma(r)} x^{(0)}(i), \quad i = 1, 2, \dots, n \tag{6}$$

2.3 A novel fractional time delay discrete model

Definition 4 Assume that the original sequence is $X^{(0)} = \{x^{(0)}(1), x^{(0)}(2), \dots, x^{(0)}(n)\}$, the r -FAO sequence of $X^{(0)}$ is $X^{(r)}$; δ_1, δ_2 and δ_3 are called undetermined parameter, then,

$$x^{(r)}(k) = \delta_1 x^{(r)}(k-1) + \delta_2 [k^{(r)} + (k-1)^{(r)}] + \delta_3, \quad k = 2, 3, \dots, n \tag{7}$$

is called Fractional Time Delay Discrete Grey Model, abbreviated as FTDDGM(1,1).

Compared with the DGM(1,1) model, the FTDDGM(1,1) model expands the order of the cumulative series to fractional order and adds a time delay term. For most data, the FTDDGM(1,1) model has stronger adaptability than the DGM(1,1) model.

are minimized, that is, the partial derivative of the loss function Q is 0, then,

$$\begin{cases} \frac{\partial Q}{\partial \delta_1} = \sum_{i=2}^n x^{(r)}(k-1) \left(x^{(r)}(k) - \delta_1 x^{(r)}(k-1) - \delta_2 \left(t^{(r)} + (t-1)^{(r)} \right) - \delta_3 \right) = 0 \\ \frac{\partial Q}{\partial \delta_2} = \sum_{i=2}^n \left(t^{(r)} + (t-1)^{(r)} \right) \left(x^{(r)}(k) - \delta_1 x^{(r)}(k-1) - \delta_2 \left(t^{(r)} + (t-1)^{(r)} \right) - \delta_3 \right) = 0 \\ \frac{\partial Q}{\partial \delta_3} = \sum_{i=2}^n \left(x^{(r)}(k) - \delta_1 x^{(r)}(k-1) - \delta_2 \left(t^{(r)} + (t-1)^{(r)} \right) - \delta_3 \right) = 0 \end{cases} \tag{10}$$

2.4 Parameter estimation

Theorem 1 Assume that $X^{(r)}$ is defined in Definition 3, the parameters vector $\hat{\delta} = (\delta_1, \delta_2, \delta_3)^T$, and

$$Y = \begin{bmatrix} x^{(r)}(2) \\ x^{(r)}(3) \\ \vdots \\ x^{(r)}(n) \end{bmatrix}, \quad B = \begin{bmatrix} x^{(r)}(1) & 1^{(r)} + 2^{(r)} & 1 \\ x^{(r)}(2) & 2^{(r)} + 3^{(r)} & 1 \\ \vdots & \vdots & \vdots \\ x^{(r)}(n-1) & (n-1)^{(r)} + n^{(r)} & 1 \end{bmatrix}.$$

Then,

$$\hat{\delta} = (\delta_1, \delta_2, \delta_3)^T = (B^T B)^{-1} B^T Y \tag{8}$$

Proof Let Eq. (3) as $Y = B \cdot \hat{\delta}$. Generally, the number of modeling data is greater than 3, that is $n > 3$. Therefore, the number of linear equations $Y = B \cdot \hat{\delta}$ is greater than the number of unknowns, Then the system of linear equations $Y = B \cdot \hat{\delta}$ has no solution. According to the least square estimation method, the error $e = Y - B \cdot \hat{\delta}$ and the loss function.

$$Q = \sum_{i=2}^n e^2 = \sum_{i=2}^n \left[x^{(r)}(k) - \delta_1 x^{(r)}(k-1) - \delta_2 \left(t^{(r)} + (t-1)^{(r)} \right) - \delta_3 \right]^2 \tag{9}$$

For Eq. (5), we have $B^T (Y - B \cdot \hat{\delta}) = 0 \Rightarrow \hat{\delta} = (B^T B)^{-1} B^T Y$.
End of proof.

2.5 Time response of fractional time delay discrete model

Theorem 2 Assume that $X^{(r)}$ and $\hat{\delta}$ as defined in Definition 4 and Theorem 1, then the time response of the fractional time delay discrete model is determined as.

$$\begin{aligned} \hat{x}^{(r)}(k) &= \delta_1^{(k-1)} x^{(r)}(1) + \sum_{i=1}^{k-1} \left[\delta_2 \left(i^{(r)} + (i+1)^{(r)} \right) + \delta_3 \right] \delta_1^{k-i-1}, \\ &k = 1, 2, \dots, n \end{aligned} \tag{11}$$

The recovery value $\hat{x}^{(0)}(k)$ is stated as

$$\begin{aligned} \hat{x}^{(0)}(k) &= \left(\hat{x}^{(r)}(k) \right)^{(-r)} \\ &= \sum_{i=0}^{k-1} (-1)^i \frac{\Gamma(r+1)}{\Gamma(i+1)\Gamma(r-i+1)} \hat{x}^{(r)}(k-i), \quad k \\ &= 1, 2, \dots, n \end{aligned} \tag{12}$$

Proof In Eq. (3), $k = 2, 3, \dots, n$, which can be obtained through iteration.

$$\begin{aligned}
 x^{(r)}(2) &= \delta_1 x^{(r)}(1) + \delta_2 (2^{(r)} + 1^{(r)}) + \delta_3 \\
 x^{(r)}(3) &= \delta_1 x^{(r)}(2) + \delta_2 (3^{(r)} + 2^{(r)}) + \delta_3 \\
 &= \delta_1 (\delta_1 x^{(r)}(1) + \delta_2 (2^{(r)} + 1^{(r)}) + \delta_3) + \delta_2 (3^{(r)} + 2^{(r)}) + \delta_3 \\
 &= \delta_1^2 x^{(r)}(1) + \delta_1 \delta_2 (2^{(r)} + 1^{(r)}) + \delta_1 \delta_3 + \delta_2 (3^{(r)} + 2^{(r)}) + \delta_3 \\
 x^{(r)}(4) &= \delta_1 x^{(r)}(3) + \delta_2 (4^{(r)} + 3^{(r)}) + \delta_3 \\
 &= \delta_1 (\delta_1^2 x^{(r)}(1) + \delta_1 \delta_2 (2^{(r)} + 1^{(r)}) + \delta_1 \delta_3 + \delta_2 (3^{(r)} + 2^{(r)}) + \delta_3) \\
 &\quad + \delta_2 (4^{(r)} + 3^{(r)}) + \delta_3 = \delta_1^3 x^{(r)}(1) + \delta_1^2 \delta_2 (2^{(r)} + 1^{(r)}) + \delta_1^2 \delta_3 \\
 &\quad + \delta_1 \delta_2 (3^{(r)} + 2^{(r)}) + \delta_1 \delta_3 + \delta_2 (4^{(r)} + 3^{(r)}) + \delta_3 \\
 &\quad \vdots \\
 x^{(r)}(k) &= \delta_1 x^{(r)}(k-1) + \delta_2 (k^{(r)} + (k-1)^{(r)}) + \delta_3 \\
 &= \delta_1^{(k-1)} x^{(r)}(1) + \delta_1^{(k-2)} \delta_2 (2^{(r)} + 1^{(r)}) + \delta_1^{(k-2)} \delta_3 + \delta_1^{(k-3)} \delta_2 (3^{(r)} + 2^{(r)}) + \delta_1^{(k-3)} \delta_3 \\
 &\quad + \delta_1^{(k-4)} \delta_2 (4^{(r)} + 3^{(r)}) + \delta_1^{(k-4)} \delta_3 + \dots + \delta_2 (k^{(r)} + (k-1)^{(r)}) + \delta_3 \\
 &= \delta_1^{(k-1)} x^{(r)}(1) + \sum_{i=1}^{k-1} (\delta_2 (i^{(r)} + (i+1)^{(r)}) + \delta_3) \delta_1^{(k-i-1)}
 \end{aligned}$$

End of proof.

2.6 The fractional time delay discrete model with variable weight buffer operator satisfies the new information priority principle

Lemma 1 Swewart (1977). Assume that $A \in C^{m \times n}$, $b \in C^m$, A^\dagger is the generalized inverse matrix of A , $B = A + E$, and $c = b + k \in C^m$. Then, $x + h$ and x satisfy the linear least squares problem that $\|Bx - c\|_2 = \min$ and $\|Ax - c\|_2 = \min$. If $\text{rank}(A) = \text{rank}(B) = n$, and $\|A^\dagger\|_2 \|E\|_2 < 1$, then.

$$\|h\| \leq \frac{\kappa_\dagger}{\gamma_\dagger} \left(\frac{\|E\|_2}{\|A\|} \|x\| + \frac{\|k\|}{\|A\|} + \frac{\kappa_\dagger \|E\|_2 \|r_x\|}{\gamma_\dagger \|A\| \|A\|} \right),$$

where $\kappa_\dagger = \|A^\dagger\|_2 \|A\|$, $\gamma_\dagger = 1 - \|A^\dagger\|_2 \|E\|$, $r_x = b - Ax$.

Theorem 3 Assume that $\hat{x}^{(0)}(k)$ is the solution of the fractional time delay discrete model. When $\hat{x}^{(0)}(k)$ is perturbed by ε , the perturbation bound is $L[x^{(0)}(k)]$. if $\varepsilon \neq 0$,

$\|B^+\|_2 \|\Delta B\|_2 \neq 0$ and $\|B^+\|_2 \|\Delta B\|_2 < 1$, then $L[x^{(0)}(n)] > L[x^{(0)}(k)]$, $k = 1, 2, \dots, n - 1$.

Proof According to Definition 2 and Definition 3, the original sequence $X^{(0)}$ is subjected to variable weight buffering operation, and then $X^{(r)}D = (x^{(r)}(1)d, x^{(r)}(2)d, \dots, x^{(r)}(n)d)$ is obtained by fractional order accumulation.

$$\begin{bmatrix} x^{(r)}(1)d \\ x^{(r)}(2)d \\ \vdots \\ x^{(r)}(n-1)d \\ x^{(r)}(n)d \end{bmatrix} = \begin{bmatrix} 1 & 0 & \dots & 0 & 0 \\ C_r^1 & 1 & \dots & 0 & 0 \\ \vdots & \vdots & \dots & \vdots & \vdots \\ C_{n+r-3}^{n-2} & C_{n+r-4}^{n-3} & \dots & 1 & 0 \\ C_{n+r-2}^{n-1} & C_{n+r-3}^{n-2} & \dots & C_r^1 & 1 \end{bmatrix} \begin{bmatrix} x^{(0)}(1) \\ x^{(0)}(2) \\ \vdots \\ x^{(0)}(n-1) \\ x^{(0)}(n) \end{bmatrix}$$

$$\begin{bmatrix} x^{(r)}(1)d \\ x^{(r)}(2)d \\ \vdots \\ x^{(r)}(n-1)d \\ x^{(r)}(n)d \end{bmatrix} = \begin{bmatrix} 1-\lambda & 0 & \cdots & 0 & \lambda \\ (1-\lambda)C_r^1 & 1-\lambda & \cdots & 0 & \lambda(1+C_r^1) \\ \vdots & \vdots & \cdots & \vdots & \vdots \\ (1-\lambda)C_{n+r-3}^{n-2} & (1-\lambda)C_{n+r-4}^{n-3} & \cdots & 1-\lambda & \lambda \sum_{i=1}^n C_{n+r-i-1}^{n-i} \\ (1-\lambda)C_{n+r-2}^{n-1} & (1-\lambda)C_{n+r-3}^{n-2} & \cdots & (1-\lambda)C_r^1 & \lambda \sum_{i=2}^n C_{n+r-i-1}^{n-i} \end{bmatrix} \begin{bmatrix} x^{(0)}(1) \\ x^{(0)}(2) \\ \vdots \\ x^{(0)}(n-1) \\ x^{(0)}(n) \end{bmatrix}$$

If $x^{(0)}(1)$ is perturbed by ε , then we have

$$\hat{Y} = Y + \Delta Y = \begin{bmatrix} x^{(r)}(2) \\ x^{(r)}(3) \\ \vdots \\ x^{(r)}(n) \end{bmatrix} + \begin{bmatrix} (1-\lambda)\varepsilon C_r^1 \\ (1-\lambda)\varepsilon C_{r+1}^2 \\ \vdots \\ (1-\lambda)\varepsilon C_{n+r-2}^{n-1} \end{bmatrix} \text{ and}$$

$$\begin{aligned} \|\Delta Y\| &= (1-\lambda)|\varepsilon|(C_r^1 + C_{r+1}^2 + \cdots + C_{n+r-2}^{n-1}) \\ &= (1-\lambda)|\varepsilon| \sum_{i=1}^{n-1} C_{n+r-i-1}^{n-i} \end{aligned}$$

$$\hat{B} = B + \Delta B = \begin{bmatrix} x^{(r)}(1) & 1^{(r)+2^{(r)}} & 1 \\ x^{(r)}(2) & 2^{(r)} + 3^{(r)} & 1 \\ \vdots & \vdots & \vdots \\ x^{(r)}(n-1) & (n-1)^{(r)} + n^{(r)} & 1 \end{bmatrix} + \begin{bmatrix} (1-\lambda)\varepsilon & 0 & 0 \\ (1-\lambda)\varepsilon C_r^1 & 0 & 0 \\ \vdots & \vdots & \vdots \\ (1-\lambda)\varepsilon C_{n+r-3}^{n-2} & 0 & 0 \end{bmatrix},$$

$$\begin{aligned} \Delta B^T \Delta B &= \begin{bmatrix} (1-\lambda)\varepsilon & (1-\lambda)\varepsilon C_r^1 & \cdots & (1-\lambda)\varepsilon C_{n+r-3}^{n-2} \\ 0 & 0 & \cdots & 0 \\ 0 & 0 & \cdots & 0 \end{bmatrix} \begin{bmatrix} (1-\lambda)\varepsilon & 0 & 0 \\ (1-\lambda)\varepsilon C_r^1 & 0 & 0 \\ \vdots & \vdots & \vdots \\ (1-\lambda)\varepsilon C_{n+r-3}^{n-2} & 0 & 0 \end{bmatrix} \\ &= \begin{bmatrix} ((1-\lambda)\varepsilon)^2 + ((1-\lambda)\varepsilon C_r^1)^2 + \cdots + ((1-\lambda)\varepsilon C_{n+r-3}^{n-2})^2 & 0 & 0 \\ 0 & 0 & 0 \\ 0 & 0 & 0 \end{bmatrix} \end{aligned}$$

$$\begin{aligned} &\sqrt{((1-\lambda)\varepsilon)^2(1 + (C_r^1)^2 + \cdots + (C_{n+r-3}^{n-2})^2)} = \\ &(1-\lambda)|\varepsilon| \sqrt{\sum_{i=2}^n (C_{n+r-i-1}^{n-i})^2} \text{ According to Lemma 1, we} \\ &\text{have} \end{aligned}$$

$$\begin{aligned} L[x^{(0)}(1)] &= (1-\lambda)|\varepsilon| \frac{\kappa_{\dagger}}{\gamma_{\dagger}} \\ &\left(\frac{\sqrt{\sum_{i=2}^n (C_{n+r-i-1}^{n-i})^2}}{\|B\|} \|x\| + \frac{\sum_{i=1}^{n-1} C_{n+r-i-1}^{n-i}}{\|B\|} + \frac{\kappa_{\dagger}}{\gamma_{\dagger}} \frac{\sqrt{\sum_{i=2}^n (C_{n+r-i-1}^{n-i})^2}}{\|B\|} \frac{\|r_x\|}{\|B\|} \right) \end{aligned}$$

If $x^{(0)}(k)$, $k = 2, 3, \dots, n-1$ is perturbed by ε , then

$$\hat{Y} = Y + \Delta Y = \begin{bmatrix} x^{(r)}(2) \\ \vdots \\ x^{(r)}(k) \\ \vdots \\ x^{(r)}(n) \end{bmatrix} + \begin{bmatrix} 0 \\ \vdots \\ (1-\lambda)\varepsilon \\ \vdots \\ (1-\lambda)\varepsilon C_{n+r-k-1}^{n-k} \end{bmatrix} \text{ and}$$

So the maximum eigenvalue of $\Delta B^T \Delta B$ is $((1-\lambda)\varepsilon)^2(1 + (C_r^1)^2 + \cdots + (C_{n+r-3}^{n-2})^2)$, then

$$\|B\|_2 = \sqrt{\lambda_{\max}(\Delta B^T \Delta B)}$$

$$\begin{aligned} \|\Delta Y\| &= (1-\lambda)|\varepsilon|(1 + C_r^1 + \cdots + C_{n+r-k-1}^{n-k}) \\ &= (1-\lambda)|\varepsilon| \sum_{i=k}^n C_{n+r-i-1}^{n-i} \end{aligned}$$

$$\hat{B} = B + \Delta B = \begin{bmatrix} x^{(r)}(1) & 1^{(r)+2^{(r)}} & 1 \\ \vdots & \vdots & \vdots \\ x^{(r)}(k) & k^{(r)} + (k+1)^{(r)} & 1 \\ \vdots & \vdots & \vdots \\ x^{(r)}(n-1) & (n-1)^{(r)} + n^{(r)} & 1 \end{bmatrix} + \begin{bmatrix} 0 & 0 & 0 \\ \vdots & \vdots & \vdots \\ (1-\lambda)\varepsilon & 0 & 0 \\ \vdots & \vdots & \vdots \\ (1-\lambda)\varepsilon C_{n+r-k-2}^{n-k-1} & 0 & 0 \end{bmatrix},$$

$$\Delta B^T \Delta B = \begin{bmatrix} 0 & \dots & (1-\lambda)\varepsilon & \dots & (1-\lambda)\varepsilon C_{n+r-k-2}^{n-k-1} \\ 0 & \dots & 0 & \dots & 0 \\ 0 & \dots & 0 & \dots & 0 \end{bmatrix}$$

$$= \begin{bmatrix} 0 & 0 & 0 \\ \vdots & \vdots & \vdots \\ (1-\lambda)\varepsilon & 0 & 0 \\ \vdots & \vdots & \vdots \\ (1-\lambda)\varepsilon C_{n+r-k-2}^{n-k-1} & 0 & 0 \\ ((1-\lambda)\varepsilon)^2 + \dots + ((1-\lambda)\varepsilon C_{n+r-k-2}^{n-k-1})^2 & 0 & 0 \\ 0 & 0 & 0 \\ 0 & 0 & 0 \end{bmatrix}.$$

So the maximum eigenvalue of $\Delta B^T \Delta B$ is $((1-\lambda)\varepsilon)^2 (1 + (C_r^1)^2 + \dots + (C_{n+r-k-2}^{n-k-1})^2)$,

then $\|B\|_2 = \sqrt{\lambda_{\max}(\Delta B^T \Delta B)} = \sqrt{((1-\lambda)\varepsilon)^2 (1 + (C_r^1)^2 + \dots + (C_{n+r-k-2}^{n-k-1})^2)}$

$(1-\lambda)|\varepsilon| \sqrt{\sum_{i=k+1}^n (C_{n+r-i-1}^{n-i})^2}$ According to Lemma 1, we

have

$$L[x^{(0)}(k)] = (1-\lambda)|\varepsilon| \frac{\kappa_{\dagger}}{\gamma_{\dagger}}$$

$$\left(\frac{\sqrt{\sum_{i=k+1}^n (C_{n+r-i-1}^{n-i})^2}}{\|B\|} \|x\| + \frac{\sum_{i=k}^n C_{n+r-i-1}^{n-i}}{\|B\|} + \frac{\kappa_{\dagger}}{\gamma_{\dagger}} \frac{\sqrt{\sum_{i=k+1}^n (C_{n+r-i-1}^{n-i})^2}}{\|B\|} \frac{\|r_x\|}{\|B\|} \right).$$

From the above formula, we can see that $L[x^{(0)}(k)]$, $k = 2, 3, \dots, n-1$ is a decreasing function, that is, under the same disturbance ε , the disturbance bound decreases gradually.

If $x^{(0)}(n)$ is perturbed by ε , then

$$\hat{Y} = Y + \Delta Y = \begin{bmatrix} x^{(r)}(2) \\ x^{(r)}(3) \\ \vdots \\ x^{(r)}(n) \end{bmatrix} + \begin{bmatrix} \lambda\varepsilon(1 + C_r^1) \\ \lambda\varepsilon(1 + C_r^1 + C_{r+1}^2) \\ \vdots \\ \lambda\varepsilon(1 + C_r^1 + C_{r+1}^2 + \dots + C_{n+r-2}^{n-1}) \end{bmatrix} \text{ and}$$

$$\|\Delta Y\| = \lambda|\varepsilon|((n-1) + (n-1)C_r^1 + (n-2)C_{r+1}^2 + \dots + C_{n+r-2}^{n-1})$$

$$= \lambda|\varepsilon| \left(n-1 + \sum_{i=1}^{n-1} i C_{n+r-i-1}^{n-i} \right).$$

$$\hat{B} = B + \Delta B = \begin{bmatrix} x^{(r)}(1) & 1^{(r)+2^{(r)}} & 1 \\ x^{(r)}(2) & 2^{(r)} + 3^{(r)} & 1 \\ \vdots & \vdots & \vdots \\ x^{(r)}(n-1) & (n-1)^{(r)} + n^{(r)} & 1 \end{bmatrix} + \begin{bmatrix} \lambda\varepsilon & 0 & 0 \\ \lambda\varepsilon(1 + C_r^1) & 0 & 0 \\ \vdots & \vdots & \vdots \\ \lambda\varepsilon(1 + C_r^1 + \dots + C_{n+r-3}^{n-2}) & 0 & 0 \end{bmatrix},$$

$$\Delta B^T \Delta B = \begin{bmatrix} \lambda\varepsilon & \lambda\varepsilon(1 + C_r^1) & \dots & \lambda\varepsilon(1 + C_r^1 + \dots + C_{n+r-3}^{n-2}) \\ 0 & 0 & \dots & 0 \\ 0 & 0 & \dots & 0 \end{bmatrix}$$

$$= \begin{bmatrix} \lambda\varepsilon & 0 & 0 \\ \lambda\varepsilon(1 + C_r^1) & 0 & 0 \\ \vdots & \vdots & \vdots \\ \lambda\varepsilon(1 + C_r^1 + \dots + C_{n+r-3}^{n-2}) & 0 & 0 \\ ((\lambda\varepsilon)^2 + (\lambda\varepsilon(1 + C_r^1))^2 + \dots + (\lambda\varepsilon(1 + C_r^1 + \dots + C_{n+r-3}^{n-2}))^2) & 0 & 0 \\ 0 & 0 & 0 \\ 0 & 0 & 0 \end{bmatrix}$$

So the maximum eigenvalue of $\Delta B^T \Delta B$ is $(\lambda\varepsilon)^2 (1 + (1 + C_r^1)^2 + \dots + (1 + C_r^1 + \dots + C_{n+r-3}^{n-2})^2)$, then

$$\begin{aligned} \|B\|_2 &= \sqrt{\lambda_{\max}(\Delta B^T \Delta B)} \\ &= \sqrt{(\lambda \varepsilon)^2 (1 + (1 + C_r^1)^2 + \dots + (1 + C_r^1 + \dots + C_{n+r-3}^{n-2})^2)} \\ &= \lambda |\varepsilon| \sqrt{\sum_{i=1}^{n-1} \left(\sum_{j=1}^i C_{i-j+r-1}^{i-j} \right)^2} \end{aligned}$$

According to Lemma 1, we have

$$\begin{aligned} L[x^{(0)}(n)] &= \lambda |\varepsilon| \frac{\kappa_{\dagger}}{\gamma_{\dagger}} \left(\frac{\sqrt{\sum_{i=1}^{n-1} \left(\sum_{j=1}^i C_{i-j+r-1}^{i-j} \right)^2}}{\|B\|} \|x\| + \frac{n-1 + \sum_{i=1}^{n-1} i C_{n+r-i-1}^{n-i}}{\|B\|} \right. \\ &\quad \left. + \frac{\kappa_{\dagger}}{\gamma_{\dagger}} \sqrt{\sum_{i=1}^{n-1} \left(\sum_{j=1}^i C_{i-j+r-1}^{i-j} \right)^2} \frac{\|r_x\|}{\|B\|} \right). \end{aligned}$$

From the expressions of $L[x^{(0)}(1)]$, $L[x^{(0)}(k)]$ and $L[x^{(0)}(n)]$, we can get $L[x^{(0)}(n)] > L[x^{(0)}(1)]$ and $L[x^{(0)}(n)] > L[x^{(0)}(k)]$, $k = 2, 3, \dots, n - 1$. That is to say, when the disturbance ε is the same, the disturbance bound of the n -th data of the new model is larger than that of the previous $n - 1$, so the new information of the n -th data has priority.

2.7 Property analysis of the FTDDGM(1,1) model

Property 1 The FTDDGM(1,1) model is compatible with the DGM(1,1) model and the FDGM(1,1) model.

Proof When the parameters $\delta_2 = 0$ and $r = 1$, Eq. (7) will become.

$$x^{(1)}(k + 1) = \beta_1 x^{(1)}(k) + \beta_2.$$

When the parameters $\delta_2 = 0$ and $r \neq 1$, Eq. (7) will become

$$x^{(r)}(k + 1) = \beta_1 x^{(r)}(k) + \beta_2.$$

Property 2 Assuming that the original sequence of the FTDDGM(1,1) model is $Z^{(0)} = \{x^{(0)}(1), x^{(0)}(2), \dots, x^{(0)}(n)\}$, and the sequence

after scaling is $Z^{(0)} = \{z^{(0)}(1), z^{(0)}(2), \dots, z^{(0)}(n)\}$, where $z^{(0)}(k) = \alpha x^{(0)}(k)$, the predicted value satisfies $\hat{z}^{(0)}(k) = \alpha \hat{x}^{(0)}(k)$.

Proof According to Eq. (6), the fractional accumulation sequence $Z^{(r)}$ of $Z^{(0)}$ is described as

$$\begin{aligned} z^{(r)}(k) &= \sum_{i=1}^k \frac{\Gamma(k+r-i)}{\Gamma(k-i+1)\Gamma(r)} z^{(0)}(i) \\ &= \alpha \sum_{i=1}^k \frac{\Gamma(k+r-i)}{\Gamma(k-i+1)\Gamma(r)} x^{(0)}(i) = \alpha x^{(r)}(k), \end{aligned}$$

then, the expressions of matrices Y_α and B_α are obtained as

$$\begin{aligned} Y_\alpha &= \begin{bmatrix} z^{(r)}(2) \\ z^{(r)}(3) \\ \vdots \\ z^{(r)}(n) \end{bmatrix} = \begin{bmatrix} \alpha x^{(r)}(2) \\ \alpha x^{(r)}(3) \\ \vdots \\ \alpha x^{(r)}(n) \end{bmatrix} = \alpha Y, \\ B_\alpha &= \begin{bmatrix} z^{(r)}(1) & 1^{(r)+2^{(r)}} & 1 \\ z^{(r)}(2) & 2^{(r)} + 3^{(r)} & 1 \\ \vdots & \vdots & \vdots \\ z^{(r)}(n-1) & (n-1)^{(r)} + n^{(r)} & 1 \end{bmatrix} = \begin{bmatrix} \alpha & 0 & 0 \\ 0 & 1 & 0 \\ 0 & 0 & 1 \end{bmatrix} \\ &\quad \begin{bmatrix} x^{(r)}(1) & 1^{(r)+2^{(r)}} & 1 \\ x^{(r)}(2) & 2^{(r)} + 3^{(r)} & 1 \\ \vdots & \vdots & \vdots \\ x^{(r)}(n-1) & (n-1)^{(r)} + n^{(r)} & 1 \end{bmatrix} = AB. \end{aligned}$$

Using least squares estimation, the parameters are determined as

$$\begin{aligned} \hat{\delta}' &= (\delta'_1, \delta'_2, \delta'_3)^T = (B_\alpha^T B_\alpha)^{-1} B_\alpha^T Y_\alpha \\ &= \alpha A^{-1} (B^T B)^{-1} B^T Y. \end{aligned}$$

Thus, there are $\delta'_1 = \delta_1$, $\delta'_2 = \alpha \delta_2$, $\delta'_3 = \alpha \delta_3$.

According to the time response of the FTDDGM(1,1) model in Eq. (11), we get

$$\begin{aligned} \hat{z}^{(r)}(k) &= \delta_1^{\alpha(k-1)} x^{(r)}(1) + \sum_{i=1}^{k-1} [\delta_2 (i^{(r)} + (i+1)^{(r)}) + \delta_3] \delta_1^{\alpha k-i-1} \\ &= \alpha \delta_1^{\alpha(k-1)} x^{(r)}(1) + \alpha \sum_{i=1}^{k-1} [\delta_2 (i^{(r)} + (i+1)^{(r)}) + \delta_3] \delta_1^{\alpha k-i-1} \\ &= \alpha \hat{x}^{(r)}(k) \end{aligned}$$

Finally, the predicted reduction value is

$$\begin{aligned} \hat{z}^{(0)}(k) &= \sum_{i=0}^{k-1} (-1)^i \frac{\Gamma(r+1)}{\Gamma(i+1)\Gamma(r-i+1)} z^{(r)}(k-i) \\ &= \alpha \sum_{i=0}^{k-1} (-1)^i \frac{\Gamma(r+1)}{\Gamma(i+1)\Gamma(r-i+1)} x^{(r)}(k-i) \\ &= \alpha \hat{x}^{(0)}(k) \end{aligned}$$

Similarly, the FTDDGM(1,1) model with variable weight buffer operator also satisfies property 2, and the proof method is similar. From property 2, it can be seen that the FTDDGM(1,1) model has scaling stability.

3 The calculation steps of the new model and the parameter optimization steps using the Grey Wolf Optimizer

It is worth noting that both the theory and the modeling process of the new model are derived under the condition that the weight λ and order r are known. Therefore, in the actual case, we need to determine the values of parameters λ and r first. In this section, the Grey Wolf Optimizer is used to optimize λ and r , and the overall calculation process of the fractional time delay discrete grey prediction model with variable weight buffer operator is shown.

3.1 FTDDGM(1,1) with variable weight buffer operator nonlinear programming

According to the modeling procedure of FTDDGM(1,1) and the definition of variable weight buffer operator, the sum of the average relative error MAPE of the model simulation reaches the minimum value, so as to find the optimal weight λ and order r in the modeling process. Assuming that the modeling number of samples is s and the prediction number is p , then we can construct the nonlinear programming of samples as

$$\min_{\lambda, r} F(\lambda, r) = \sum_{k=1}^s \left| \frac{\hat{x}^{(0)}(k) - x^{(0)}(k)}{x^{(0)}(k)} \right| \times 100\% \tag{14}$$

$$\begin{cases} B = \begin{bmatrix} x^{(r)}(1)d & 1^{(r)+2^{(r)}} & 1 \\ x^{(r)}(2)d & 2^{(r)+3^{(r)}} & 1 \\ \vdots & \vdots & \vdots \\ x^{(r)}(s-1)d & (s-1)^{(r)+s^{(r)}} & 1 \end{bmatrix}, Y = \begin{bmatrix} x^{(r)}(2) \\ x^{(r)}(3) \\ \vdots \\ x^{(r)}(s) \end{bmatrix} \\ \hat{\delta} = (\delta_1, \delta_2, \delta_3)^T = (B^T B)^{-1} B^T Y \\ \hat{x}^{(r)}(k)d = \delta_1^{(k-1)} x^{(r)}(1) \\ + \sum_{i=1}^{k-1} [\delta_2(i^{(r)} + (i+1)^{(r)}) + \delta_3] \delta_1^{k-i-1}, i = 1, 2, \dots, s \\ \hat{X}^{(0)}(k)d = (\hat{X}_1^{(r)}(k))^{(-r)} \\ = \sum_{i=1}^k \binom{k-i-r-1}{k-i} \hat{X}^{(0)}(i)d, k = 1, 2, \dots, s+p \\ \hat{X}^{(0)}(k) = \frac{(\hat{X}^{(0)}(k)d - \lambda \hat{X}^{(0)}(s)d)}{1-\lambda}, k = 1, 2, \dots, s \\ \hat{X}^{(0)}(k) = \hat{X}^{(0)}(k)d, k = s+1, \dots, s+p \end{cases}$$

3.2 Grey Wolf Optimizer (GWO)

The grey wolf optimizer was proposed by Mirjalili et al. (2014), which has the characteristics of fast convergence speed and strong optimization ability. By simulating the preying behaviour of grey wolves, the steps of social hierarchy, searching for prey, encircling and attacking prey are included. According to the fitness of the individual, the grey wolf population was assigned a social ranking of fitness from highest to lowest, α , β , δ and ω . The position information of the current three optimal solutions α , β and δ is used to update the position of other search agents. The iterative formula is as follows:

$$\begin{cases} \vec{D}_\alpha = |\vec{C}_1 \cdot \vec{X}_\alpha - \vec{X}|, \vec{D}_\beta = |\vec{C}_2 \cdot \vec{X}_\beta - \vec{X}|, \vec{D}_\delta = |\vec{C}_3 \cdot \vec{X}_\delta - \vec{X}| \\ \vec{X}_1 = \vec{X}_\alpha - \vec{A}_1 \cdot \vec{D}_\alpha, \vec{X}_2 = \vec{X}_\beta - \vec{A}_2 \cdot \vec{D}_\beta, \vec{X}_3 = \vec{X}_\delta - \vec{A}_3 \cdot \vec{D}_\delta \\ \vec{X}(t+1) = \frac{\vec{X}_1 + \vec{X}_2 + \vec{X}_3}{3} \end{cases} \tag{15}$$

where \vec{X}_α , \vec{X}_β , and \vec{X}_δ represent the position vectors of α , β and δ ; \vec{D}_α , \vec{D}_β and \vec{D}_δ represent the distance between the current individual and α , β , and δ ; \vec{X} represents the position vector of the grey wolf.

The vectors \vec{A} and \vec{C} are calculated as follows:

$$\vec{A} = 2\vec{a} \cdot \vec{r}_1 - \vec{a}, \vec{C} = 2 \cdot \vec{r}_2$$

where \vec{a} is linearly reduced from 2 to 0 in the iteration process, \vec{r}_1 and \vec{r}_2 are random vectors between $[0, 1]$.

3.3 The parameter optimization and the calculation steps

The GWO is used to optimize the order r of the new model and the weight λ of the buffer operator. The specific steps are shown in the source code of Algorithm 1.

Algorithm 1 The parameter optimization**Input:** The initial sequence $X^{(0)} = \{x^{(0)}(1), x^{(0)}(2), \dots, x^{(0)}(n)\}$ **Output:** The optimal weight λ and the optimal order r of the buffer operator

- 1: **Initialize** the number of grey wolf populations
- 2: **Initialize** the vector a , A and C
- 3: **Initialize** the X_α , X_β , X_δ , and calculate the fitness of each individual according to Eq. (9)
- 4: **Set** the maximum number of iterations
- 5: **for** $t < \text{Max_iter}$ **do**
- 6: **for** each search agent **do**
- 7: **Update** the current agent location according to Eq. (11)
- 8: **end for**
- 9: Update the vectors a , A and C
- 10: **for** each search agent **do**
- 11: Calculate the $(x^{(r)}(1)d, x^{(r)}(2)d, \dots, x^{(r)}(n)d)$ according to Eq. (1) and Eq. (2)
- 12: Calculate the $\hat{\delta} = (\delta_1, \delta_2, \delta_3)^T$ according to **Theorem 1**
- 13: Calculate the $\hat{x}^{(0)}(k)$ according to Eq. (10)
- 14: **end for**
- 15: Calculate the fitness according to Eq. (9) and update X_α , X_β and X_δ
- 16: **end for**

4 Applications

This section first introduces the evaluation criteria of the model and then uses the data of solar renewable energy consumption, total biomass renewable energy consumption and wind renewable energy consumption in the USA to build the grey prediction model, which verifies the effectiveness of FTDDGM(1,1) model with variable weight buffer operator. Finally, FTDDGM(1,1) model with variable weight buffer operator is used to predict the solar renewable energy consumption, total biomass renewable

energy consumption and wind renewable energy consumption in the USA from 2020 to 2024.

4.1 Evaluation criteria

In order to verify the prediction effect of the new model in practical application, this section selects three cases of renewable energy consumption in the USA to analyse the performance of the FTDDGM(1,1) model and compares it with the other five models. The relative percentage error ($\Delta(k)$) and the mean absolute percentage error (MAPE)

Table 1 Abbreviation of grey model in this paper

Abbreviation	Expression	Meaning
GM(1,1)	$\frac{dx^{(1)}(t)}{dt} + ax^{(1)}(t) = b$	Basic grey model
GM(1,n)	$\frac{dx^{(1)}(t)}{dt} + aX_1^{(1)}(t) = \sum_{j=2}^n b_j X_j^{(1)}(t)$	Basic multivariate grey model
DGM(1,1)	$x^{(1)}(k + 1) = \beta_1 x^{(1)}(k) + \beta_2$	Discrete GM(1,1) model
FGM(1,1)	$\frac{dx^{(r)}(t)}{dt} + ax^{(r)}(t) = b$	Fractional-order GM(1,1) model
FDGM(1,1)	$x^{(r)}(k + 1) = \beta_1 x^{(r)}(k) + \beta_2$	Fractional-order discrete GM(1,1) model
Verhulst	$\frac{dx^{(1)}(t)}{dt} + ax^{(1)}(t) = b(x^{(1)}(t))^2$	Single sequence first-order nonlinear dynamic model
N_Verhulst	$\frac{dy^{(1)}(t)}{dt} + ay^{(1)}(t) = \frac{1}{2}(2t - 1)b + c$	New grey Verhulst model

Table 2 Solar renewable energy consumption of the USA from 2009 to 2019

Year	2009	2010	2011	2012	2013	2014	2015	2016	2017	2018	2019
Consumption	78	91	112	159	225	338	427	570	777	916	1018

were used as the evaluation criteria. The expression is described as

$$\Delta(k) = \left| \frac{x^{(0)}(k) - \hat{x}^{(0)}(k)}{x^{(0)}(k)} \right| \times 100\%, \quad k = 1, 2, \dots, n \quad (16)$$

$$MAPE_s = \frac{1}{s} \times \sum_{k=1}^s \left| \frac{\hat{x}^{(0)}(k) - x^{(0)}(k)}{x^{(0)}(k)} \right| \times 100\% \quad (17)$$

$$MAPE_p = \frac{1}{n - s} \times \sum_{k=s+1}^n \left| \frac{\hat{x}^{(0)}(k) - x^{(0)}(k)}{x^{(0)}(k)} \right| \times 100\% \quad (18)$$

where n is the total number of samples, s is the number of models, MAPEs is the mean absolute percentage error of model simulation, and MAPEp is the mean absolute percentage error of model prediction. Table 1 is the abbreviation of grey model in this paper.

4.2 Case analysis

This section will illustrate the effectiveness of FTDDGM(1,1) model with variable weight buffer operator from three aspects. Firstly, the actual data of solar renewable energy consumption, total biomass renewable energy consumption and wind renewable energy consumption in the USA are used to build the prediction model. Secondly, the prediction accuracy is compared with the existing grey model. Finally, in case 1 and case 2, the data from 2009 to 2015 were used as the training set to establish the model, and the data from 2016 to 2019 were used as the test set to compare the prediction performance. In case 3, In case 3, set the parameter $\lambda = 0$ of the variable weight buffer operator,

and the data from 2006 to 2015 was used as the training set, and the data from 2016 to 2019 was used as the test set.

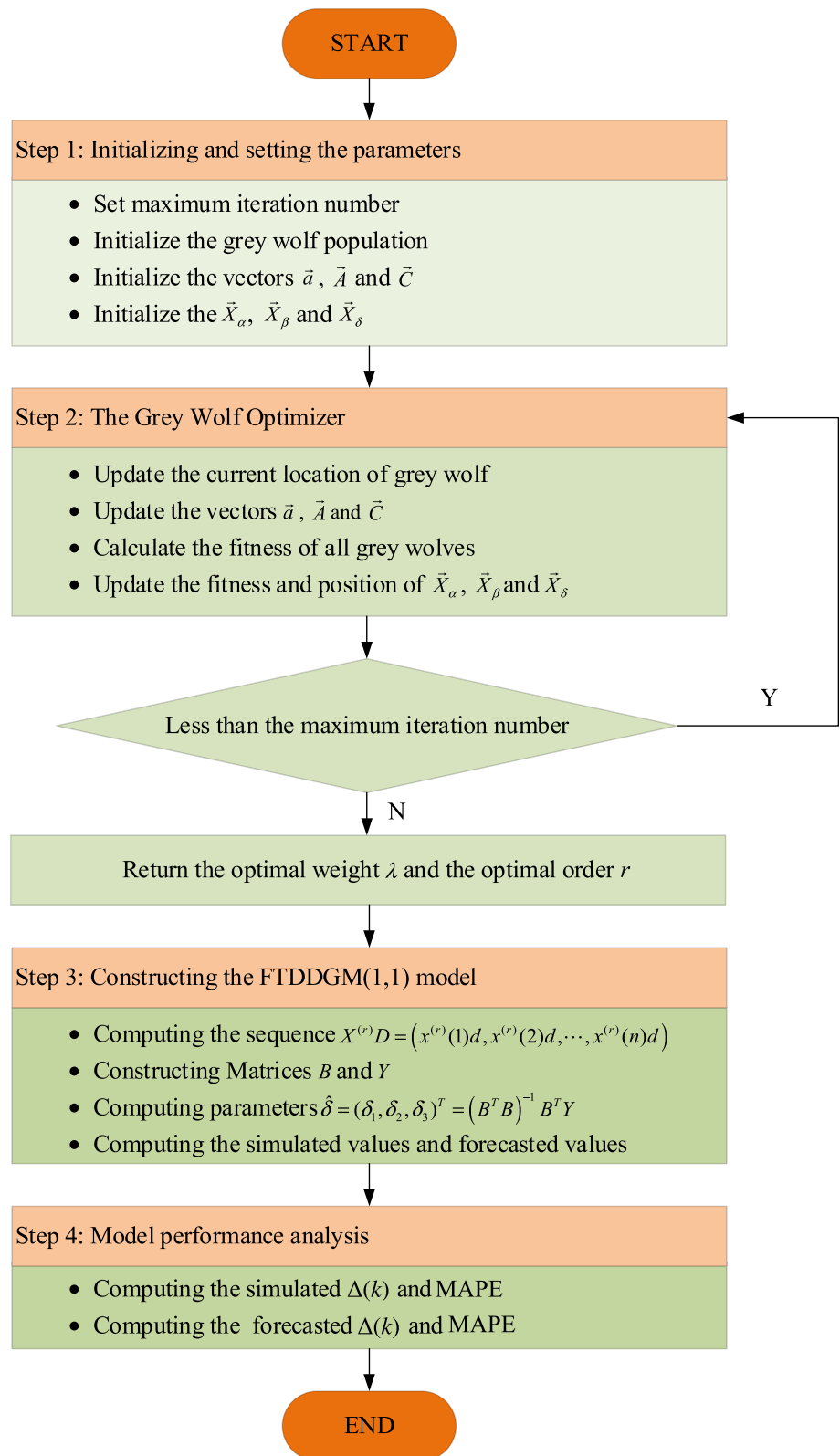
Case 1 The solar renewable energy consumption of the USA.

In this case, the consumption of solar energy in the USA from 2009 to 2015 recorded by the US Energy Information Administration (EIA) is shown in Table 2 (<https://www.eia.gov/totalenergy/data/browser/?tbl=T10.01#/>). Data from 2009 to 2015 were set as modeling data for model training, and data from 2016 to 2019 were set as prediction data for model prediction performance analysis (Fig. 1).

In order to clearly observe the effect of the buffer operator on processing the original data, we substituted the modeling data in Case 1 into Eq. (1) to get the values under different weights, and drew the curves as shown in Fig. 2. When $\lambda = 0$, the curve acted by the variable weight buffer operator coincides with the curve of the original data, that is, the FTDDGM(1,1) model uses the original data for modeling. As λ increases from 0 to 1, the rate of change of data decreases, and the growth rate of data gradually tends to be flat.

The Grey Wolf Optimizer is used to search the optimal weight λ and the optimal order r , and the search process is shown in Fig. 3. According to the calculation process of FTDDGM(1,1) with variable weight buffer operator in Fig. 1, the parameter values of Case 1 are shown in Table 3. At this time, the weight is $\lambda = 0.00044734$, and the effect of the buffer operator is relatively small. At the same time, the simulation and prediction data were obtained and the relative percentage errors of each year

Fig. 1 Flow chart of FTDDGM(1,1) with variable weight buffer operator



were calculated. The mean absolute percentage errors of the simulation and prediction are shown in Table 4. The simulation and prediction mean absolute percentage errors

of the six models are plotted as a column chart, as shown in Fig. 4, and the broken line chart of the six models in Case 1

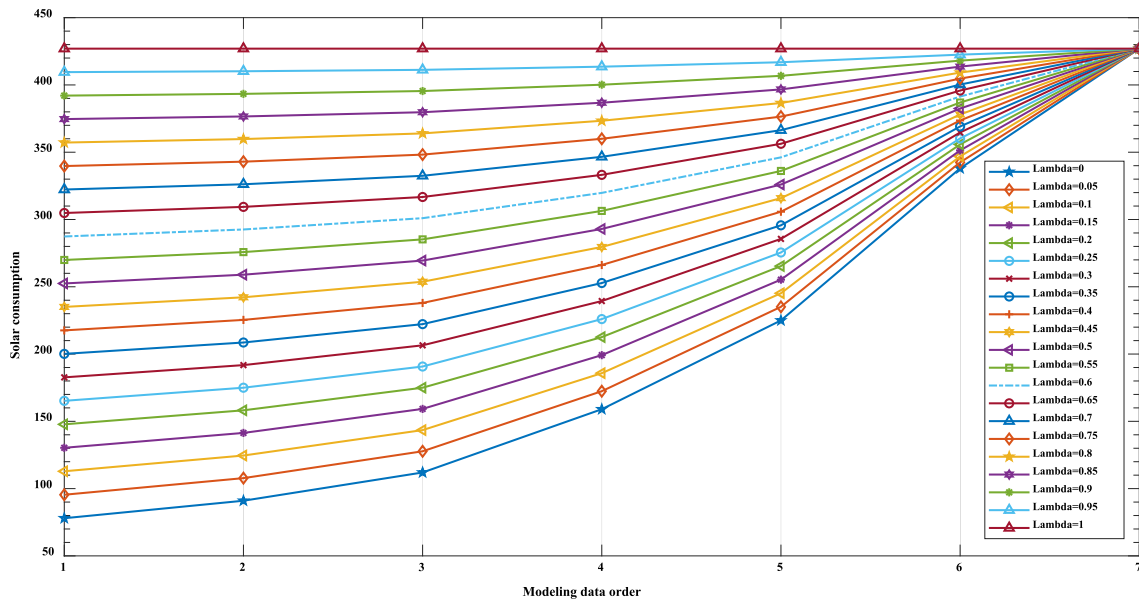


Fig. 2 The effect diagram of the modeling data of Case 1 in the buffer operator with different weights

Fig. 3 The three-dimensional search graph of the best weight λ and order r of the FTDDGM(1,1) model is in Case 1

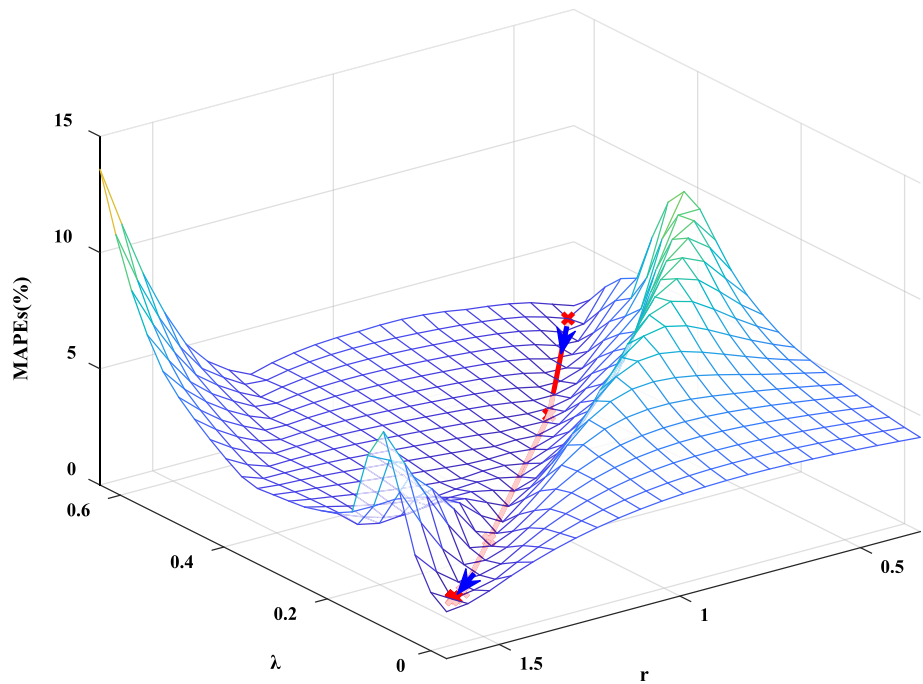


Table 3 The parameter values of FTDDGM(1,1) with variable weight buffer operator in Case 1

λ	r	δ_1	δ_2	δ_3
0.00044734	1.5864	0.9782	8.93618	97.7022

is drawn in combination with Fig. 5 to visually analyse and compare the performance of the six models.

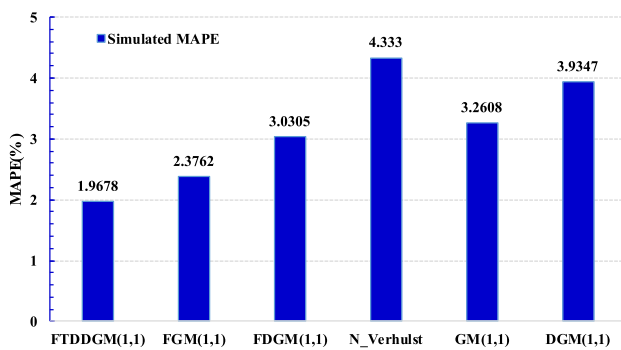
In particular, because the prediction effect of N_Verhulst model in Case 1 is not good, which affects the display

effect of other models, the line chart of N_Verhulst model is not shown in Fig. 5.

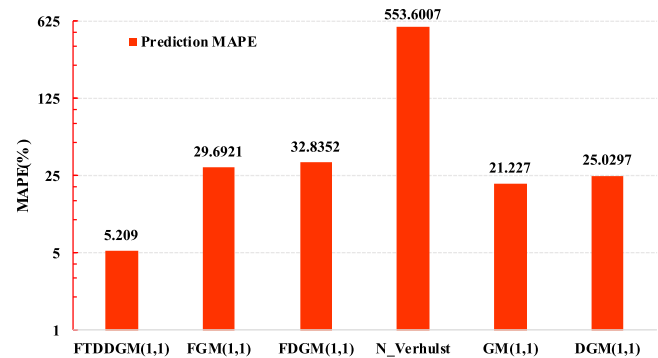
Through Table 4, Figs. 4 and 5, the simulation and prediction effects of the six models in Case 1 are intuitively displayed. It can be clearly seen that the FTDDGM(1,1) model has a lower simulation MAPE value than the other five models in the case, and has the best fitting effect with the original data. Of course, we mainly focus on the prediction effect of FTDDGM(1,1) model. The prediction MAPE value of the FTDDGM(1,1) model is much lower

Table 4 The Simulation and prediction data of six models in Case 1

Year	z	FTDDGM(1,1)		FGM(1,1)		FDGM(1,1)		N_Verhulst		GM(1,1)		DGM(1,1)	
		$\hat{x}^{(0)}(k)$	$\Delta(k)$										
<i>Simulation</i>													
2009	78	78	0	78	0	78	0	78	0	78	0	78	0
2010	91	91	0	91	0	91	0	89.27	1.9	85.8	5.71	86.95	4.45
2011	112	108.61	3.03	117.02	4.48	119.57	6.76	117.69	5.08	118.39	5.71	120.25	7.37
2012	159	161.4	1.51	159.4	0.25	163.69	2.95	157.93	0.68	163.36	2.74	166.3	4.59
2013	225	234.33	4.15	221.2	1.69	227.43	1.08	217.43	3.36	225.41	0.18	229.99	2.22
2014	338	324.95	3.86	309.42	8.46	318.09	5.89	311.33	7.89	311.02	7.98	318.08	5.89
2015	427	432.22	1.22	434.5	1.76	446.35	4.53	475.77	11.42	429.14	0.5	439.89	3.02
MAPEs		1.9678		2.3762		3.0305		4.333		3.2608		3.9347	
<i>Prediction</i>													
2016	570	555.42	2.56	611.37	7.26	627.43	10.08	824.21	44.6	592.13	3.88	608.37	6.73
2017	777	694.11	10.67	861.22	10.84	882.84	13.62	1991.71	156.33	817.03	5.15	841.36	8.28
2018	916	847.85	7.44	1213.93	32.52	1242.93	35.69	- 14,890	1725.57	1127.34	23.07	1163.58	27.03
2019	1018	1016.27	0.17	1711.73	68.15	1750.48	71.95	- 1912.9	287.91	1555.51	52.8	1609.22	58.08
MAPEp		5.209		29.6921		32.8352		553.6007		21.227		25.0297	



(a)



(b)

Fig. 4 Comparison of the simulation and prediction mean relative errors between FTDDGM(1,1) and other five models in Case 1. **a** is the MAPE value of six models simulation; **b** represents the MAPE values prediction by the six models

than the other five models, and the prediction effect is the best. Therefore, the FTDDGM(1,1) model showed high performance in Case 1. Figure 6 shows the effect diagram of the training data of Case 2 in different weight buffer operators.

Case 2 The total biomass renewable energy consumption of the USA.

In this case, the total biomass renewable energy consumption of the USA from 2009 to 2019 recorded in the US Energy Information Administration (EIA) is shown in Table 5 (Wang et al. 2022g). The training data from 2009 to 2015 were used for modeling, and the test data from 2016 to 2019 were used for model performance comparison.

The training data in Case 2 is buffered according to definition 2. The effect of changing λ from 0 to 1 with step size of 0.5 is shown in Fig. 5. Combined with algorithm 1, the parameters of FTDDGM(1,1) model in Case 2 are optimized. The three-dimensional search diagram is shown in Fig. 7.

The Grey Wolf Optimizer is used to search for the optimal weight λ and order r , then we can calculate matrix B and matrix Y . Therefore, combining formula 4, we can get the FTDDGM(1,1) model with variable weight buffer operator in Case 2 each The values of the parameters are shown in Table 6. It can be seen that the searched optimal weight $\lambda=0.97599$, so the buffer operator has a strong effect on FTDDGM(1,1).

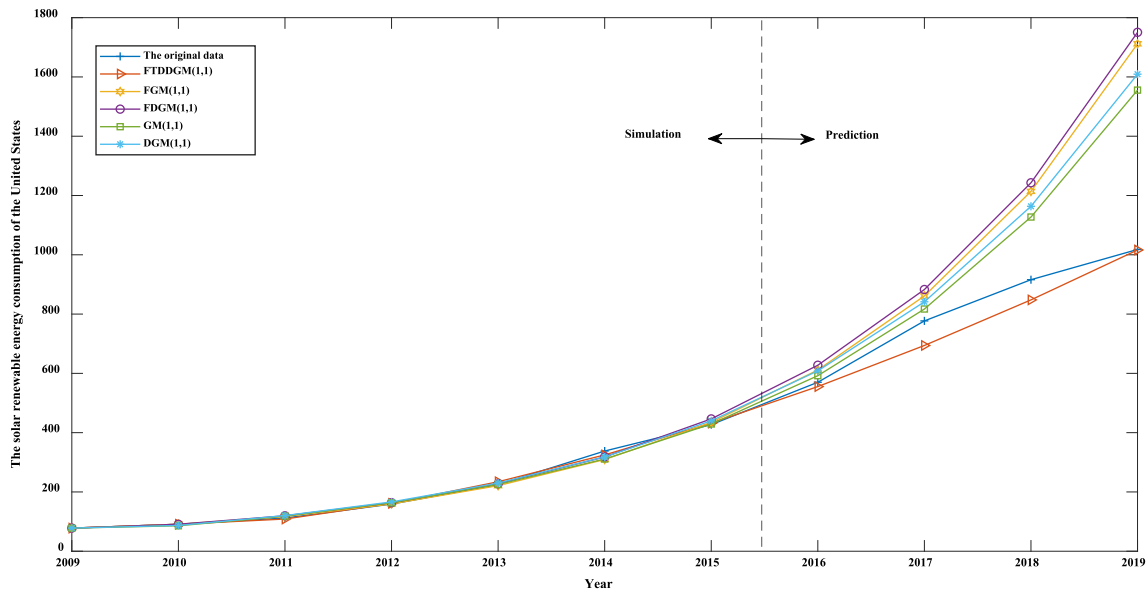


Fig. 5 The simulation and prediction line charts of the six models in Case 1

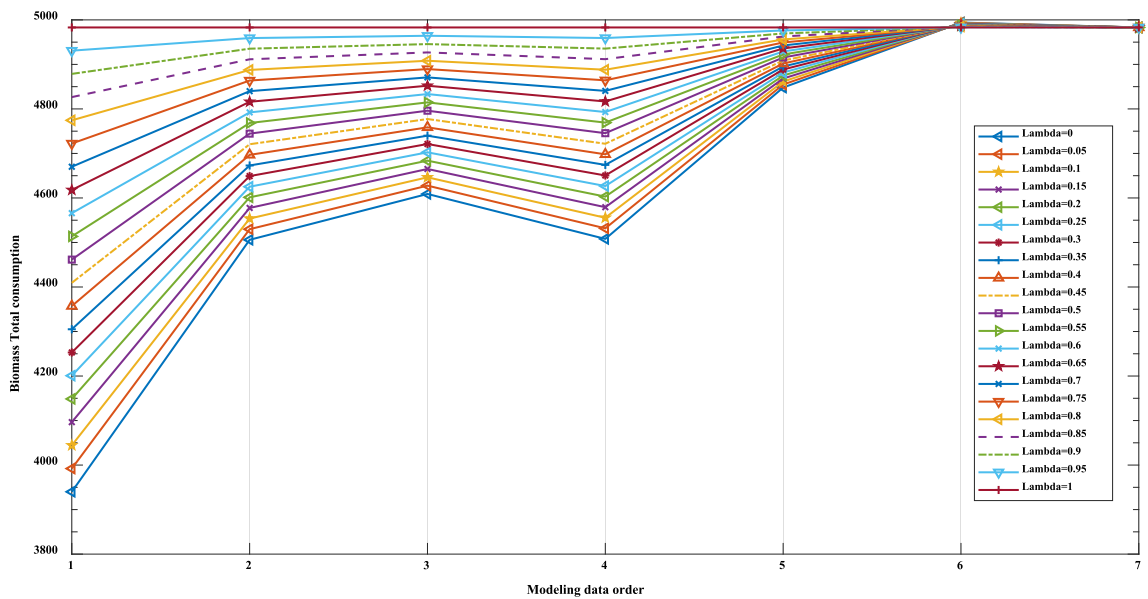


Fig. 6 The effect diagram of the training data of Case 2 in different weight buffer operators

Table 5 Total biomass renewable energy consumption of the USA

Year	2009	2010	2011	2012	2013	2014	2015	2016	2017	2018	2019
Consumption	3940	4506	4609	4508	4848	4994	4983	5015	4979	5031	4924

According to Eq. (10), the simulation value and the prediction value in Case 2 are calculated, and the relative percentage error and average relative error of each year are calculated and statistics are shown in Table 7. In order to more intuitively compare the prediction effect of the six models in the Case 2, the simulation of various models and

the average relative error of prediction are drawn into a bar graph, as shown in Fig. 8. At the same time, the simulation and prediction values of the six models in each year are drawn into a line chart, as shown in Fig. 9.

According to Table 7, Figs. 8 and 9, we can draw obvious conclusions through data and charts. In Case 2, the

Fig. 7 The three-dimensional search graph of the best weight λ and the order r of the FTDDGM(1,1) model is in Case 2

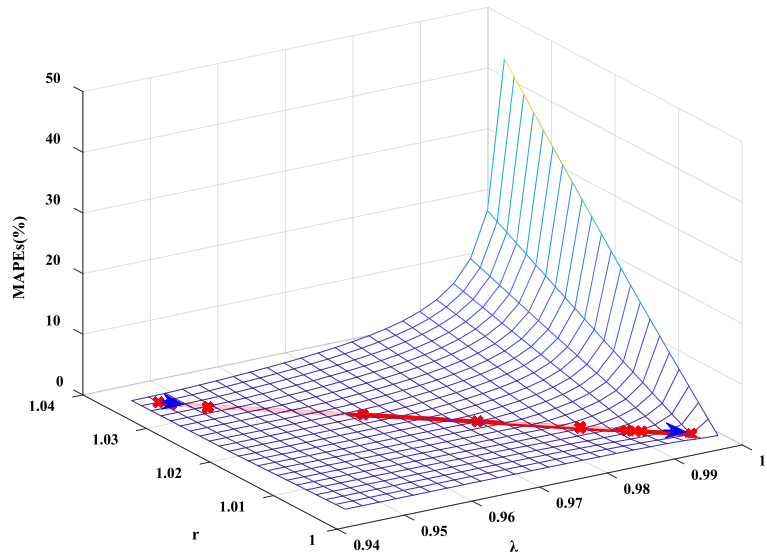


Table 6 The parameter values of FTDDGM(1,1) with variable weight buffer operator in Case 2

λ	r	δ_1	δ_2	δ_3
0.97599	1.0149	1.0097	- 2.7849	5009.8482

simulation MAPE value of FTDDGM(1,1) is only 1.1386%, which is less than that of the other five models. In particular, the significant effect of FTDDGM(1,1) in the prediction of Case 2. The numerically prediction MAPE value is only 0.6627%, which is much lower than the other

five models. At the same time, we can see that the FTDDGM(1,1) model and the variable weight buffer operator have a strong correlation with the test data. Therefore, in the prediction of Case 2, the prediction performance of the FTDDGM(1,1) model and the variable weight buffer operator is better than the other five models.

Case 3 The wind renewable energy consumption of the USA.

In order to verify the prediction performance of the FTDDGM(1,1) model when the buffer operator weight $\lambda=0$. In this case, the consumption of wind energy in the

Table 7 The Simulation and prediction data of six models in Case 2

Year	FTDDGM(1,1)		FGM(1,1)		FDGM(1,1)		N_Verhulst		GM(1,1)		DGM(1,1)		
	$x^{(0)}(k)$	$x^{(0)}(k)$	$\Delta(k)$										
<i>Simulation</i>													
2009	3940	3940	0	3940	0	3940	0	3940	0	3940	0	3940	0
2010	4506	4564.84	1.31	4506.05	0	4506	0	4462.98	0.95	4467.54	0.85	4468.43	0.83
2011	4609	4450.37	3.44	4557.66	1.11	4558.97	1.09	4576.27	0.71	4573.54	0.77	4574.2	0.76
2012	4508	4631.23	2.73	4654.03	3.24	4655.48	3.27	4687.7	3.99	4682.06	3.86	4682.46	3.87
2013	4848	4841.52	0.13	4772.46	1.56	4773.5	1.54	4797.09	1.05	4793.15	1.13	4793.29	1.13
2014	4994	4976.37	0.35	4905.69	1.77	4905.97	1.76	4904.25	1.8	4906.88	1.74	4906.74	1.75
2015	4983	4983	0	5050.5	1.35	5049.77	1.34	5009.04	0.52	5023.31	0.81	5022.87	0.8
MAPEs		1.1386		1.2908		1.2852		1.2887		1.3098		1.305	
<i>Prediction</i>													
2016	5015	4979.34	0.71	5205.27	3.79	5203.31	3.75	5111.31	1.92	5142.49	2.54	5141.76	2.53
2017	4979	4971.39	0.15	5369.09	7.83	5365.71	7.77	5210.94	4.66	5264.51	5.73	5263.46	5.71
2018	5031	4958.8	1.44	5541.49	10.15	5536.5	10.05	5307.83	5.5	5389.42	7.12	5388.03	7.1
2019	4924	4941.33	0.35	5722.2	16.21	5715.44	16.07	5401.88	9.71	5517.3	12.05	5515.56	12.01
MAPEp		0.66274		9.4965		9.4106		5.4466		6.8625		6.8378	

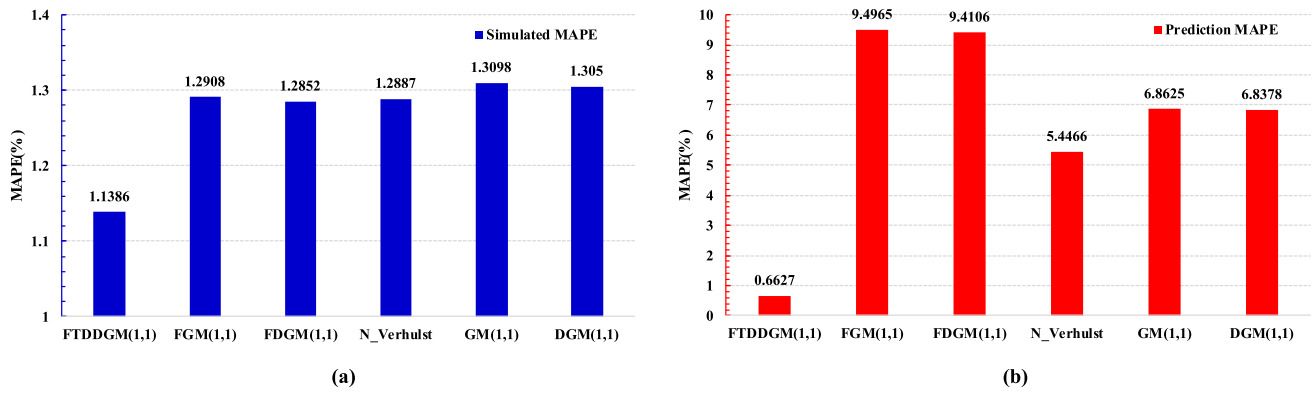


Fig. 8 Comparison of the simulation and prediction mean relative errors between FTDDGM(1,1) and other five models in Case 2. **a** is the MAPE value of six models simulation; **b** represents the MAPE values prediction by the six models

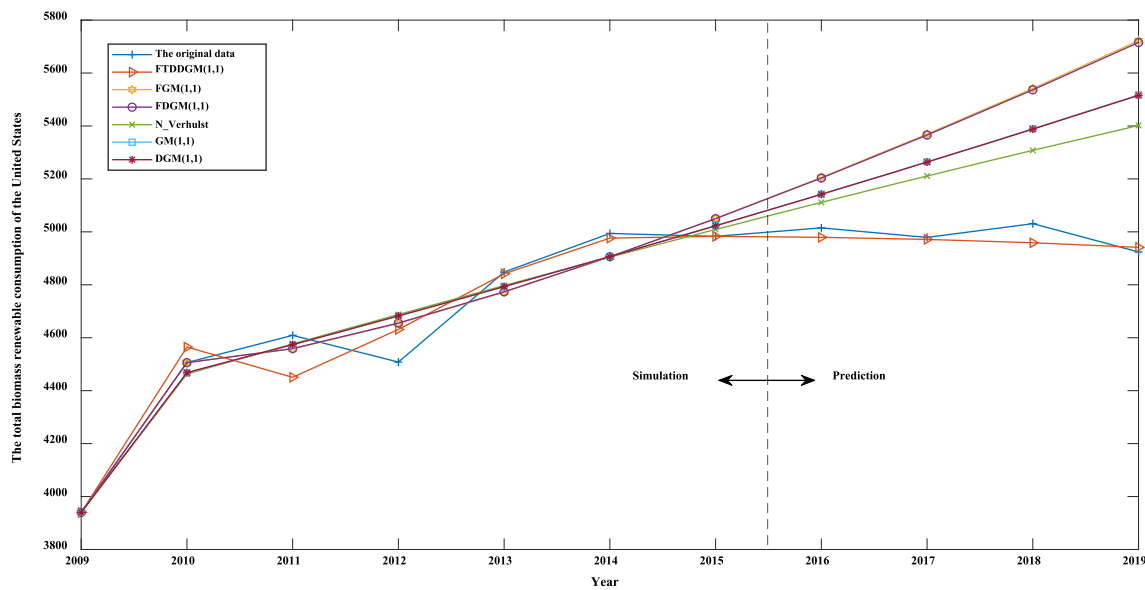


Fig. 9 The simulation and prediction line charts of the six models in Case 2

Table 8 Wind energy consumption of the USA

Year	2006	2007	2008	2009	2010	2011	2012
Consumption	264	341	546	721	923	1168	1340
Year	2013	2014	2015	2016	2017	2018	2019
Consumption	1601	1728	1777	2096	2343	2482	2626

USA from 2006 to 2019 recorded in the US Energy Information Administration (EIA) is shown in Table 8 (Wang et al. 2022g). The data from 2006 to 2015 were modeling and the data from 2016 to 2019 were compared to the model prediction performance.

We set $\lambda = 0$, and Case 3 just searches for order r . The Algorithm 1 is used to optimize the order of FTDDGM(1,1) model, and the iteration process is shown in Fig. 10. Then, the searched optimal order r and weight

$\lambda = 0$ were substituted into Eq. (4), and the relevant parameters of the model are obtained in Table 9.

At this time, the simulation values and prediction values of Case 3 were obtained by the modeling process of FTDDGM(1,1) model. The statistics of data of each year are shown in Table 10, and the simulation MAPE values and prediction MAPE values are drawn into a bar graph in Fig. 11. Finally, in order to clearly compare the effects of each model, the simulation values and prediction values of the six models in Case 3 were drawn into a line chart, as shown in Fig. 12.

Through the presentation of numerical results in Table 10, we can clearly see that the relative percentage error in the simulation and prediction of the FTDDGM(1,1) model in Case 3 is small. Combined with Fig. 11, it can be concluded that both FTDDGM(1,1) model and N_Verhulst model show good fitting effect, but the simulation MAPE

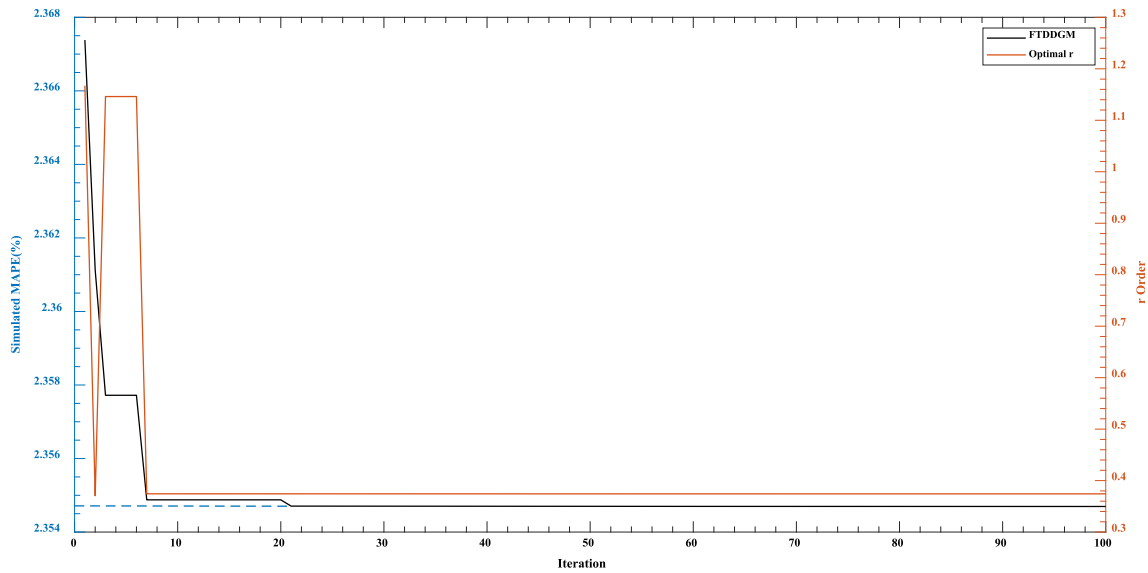


Fig. 10 The optimal order r iteration process of FTDDGM(1,1) model in Case 3

Table 9 The parameter values of FTDDGM(1,1) in Case 3

λ	r	δ_1	δ_2	δ_3
0	0.37421	- 0.1231	110.2808	100.1960

value of FTDDGM(1,1) model is lower and the fitting effect is better. The most noteworthy is the prediction effect of FTDDGM(1,1), the prediction MAPE value is only 1.4111%. It can be clearly seen from Fig. 12 that the prediction curve of FTDDGM(1,1) and FGM(1,1) is close

Table 10 The simulation and prediction data of six models in Case 3

Year	FTDDGM(1,1)		FGM(1,1)		FDGM(1,1)		N_Verhulst		GM(1,1)		DGM(1,1)		
	$x^{(0)}(k)$	$\Delta(k)$											
<i>Simulation</i>													
2006	264	0	264	0	264	0	264	0	264	0	264	0	
2007	341	0	429.01	25.81	448.84	31.63	346.27	1.54	567.06	66.29	572.48	67.88	
2008	546	1.48	598.67	9.65	629.16	15.23	516.26	5.45	664.8	21.76	670.65	22.83	
2009	721	3.32	773.12	7.23	805.11	11.67	728.99	1.11	779.4	8.1	785.67	8.97	
2010	923	1.73	952.49	3.2	976.86	5.83	965.45	4.6	913.75	1	920.4	0.28	
2011	1168	2.98	1136.92	2.66	1144.54	2.01	1196.05	2.4	1071.25	8.28	1078.25	7.68	
2012	1340	0.9	1326.55	1	1308.28	2.37	1393.96	4.03	1255.91	6.28	1263.16	5.73	
2013	1601	4.88	1521.52	4.96	1468.21	8.29	1546.02	3.43	1472.39	8.03	1479.79	7.57	
2014	1728	0.58	1722	0.35	1624.41	5.99	1653.21	4.33	1726.19	0.1	1733.56	0.32	
2015	1777	7.67	1928.13	8.5	1777	0	1724.27	2.97	2023.74	13.89	2030.85	14.29	
MAPEs	2.3547		6.3362	8.3023	2.9856		13.3736	13.556					
<i>Prediction</i>													
2016	2096	0.61	2140.07	2.1	1926.06	8.11	1769.48	15.58	2372.58	13.2	2379.13	13.51	
2017	2343	1.65	2357.99	0.64	2071.69	11.58	1797.5	23.28	2781.55	18.72	2787.14	18.96	
2018	2482	0.73	2582.06	4.03	2213.97	10.8	1814.57	26.89	3261.02	31.39	3265.11	31.55	
2019	2626	2.66	2812.44	7.1	2352.97	10.4	1824.88	30.51	3823.13	45.59	3825.06	45.66	
MAPEp	1.4111		3.4684		10.2209		24.0646		27.2219		27.4193		

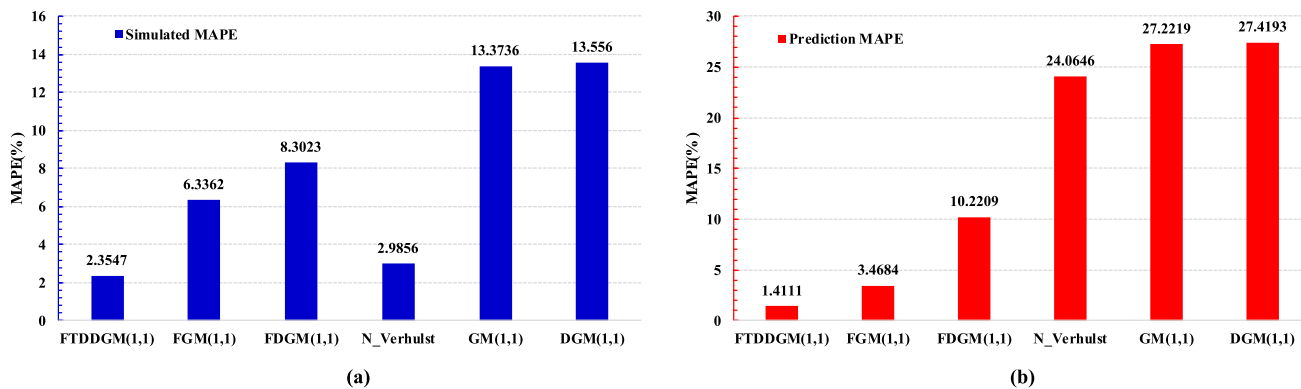


Fig. 11 Comparison of the simulation and prediction mean relative errors between FTDDGM(1,1) and other five models in Case 3. **a** is the MAPE value of six models simulation; **b** represents the MAPE values prediction by the six models

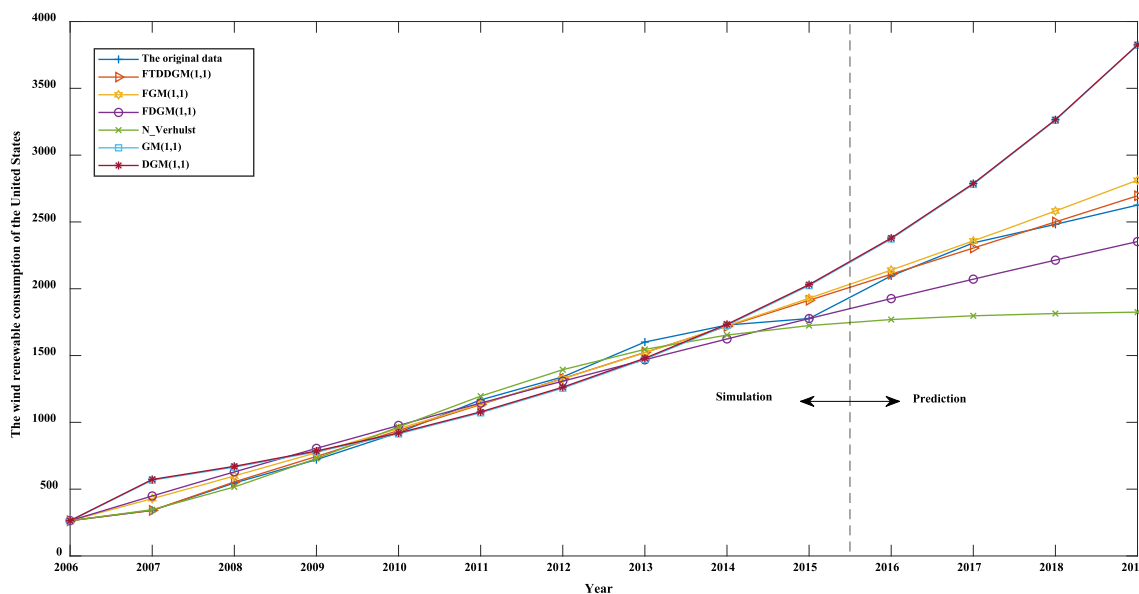


Fig. 12 The simulation and prediction line charts of the six models in Case 3

Table 11 Forecast data of solar renewable energy consumption in the USA from 2020 to 2024

Year	2020	2021	2022	2023	2024
Consumption	1199.00	1395.72	1606.09	1829.80	2066.56

to the original curve. By comparing the prediction curve of FTDDGM(1,1) and FGM(1,1), we find that the prediction curve of FTDDGM(1,1) is closer to the original data. Therefore, the prediction effect and performance of FTDDGM(1,1) in Case 3 are the best among the six models.

4.3 Forecast research

According to the case analysis in Sect. 4.2, the FTDDGM(1,1) model with variable weight buffer operator shows better prediction performance in solar renewable energy consumption, total biomass renewable energy consumption and wind renewable energy consumption in the USA. Therefore, in this section, FTDDGM(1,1) model with variable weight buffer operator is used to predict solar renewable energy consumption, total biomass renewable energy consumption and wind renewable energy consumption in the USA from 2020 to 2024.

Case 1 Forecast of solar renewable energy consumption of the USA from 2020 to 2024.

In this case, the prediction method of case 1 in Sect. 4.2 will continue to be used. The USA solar renewable energy

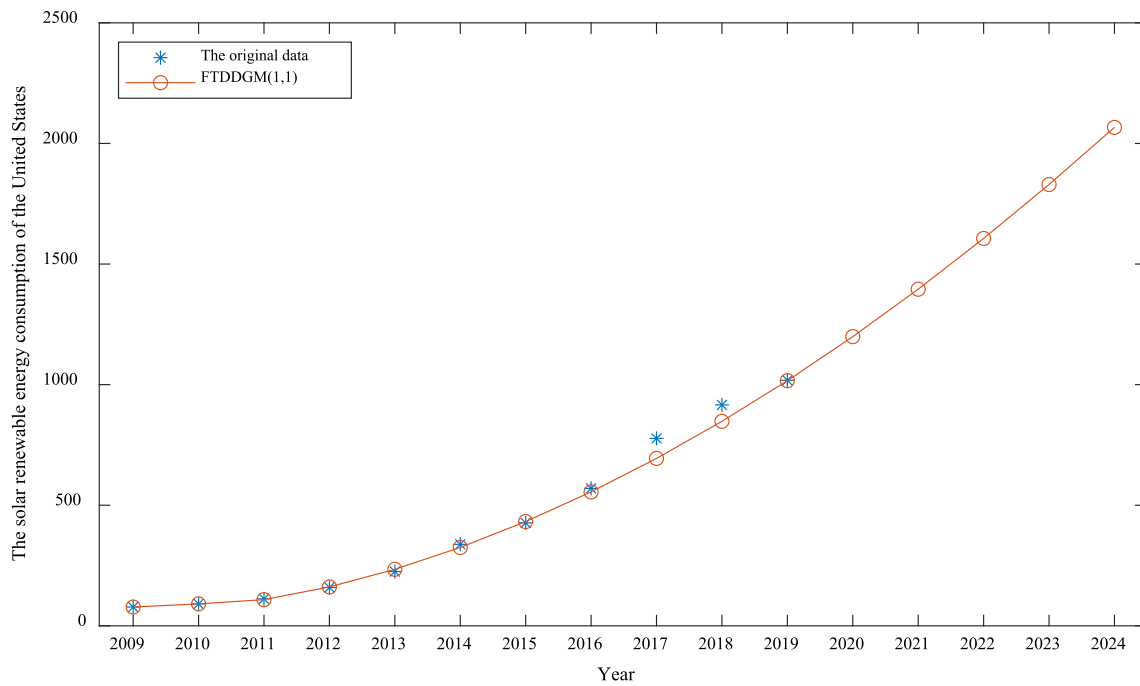


Fig. 13 Prediction trend of FTDDGM(1,1) with variable weight buffer in Case 1

Table 12 Forecast data of total biomass renewable energy consumption in the USA from 2020 to 2024

Year	2020	2021	2022	2023	2024
Consumption	4918.78	4890.99	4857.83	4819.17	4774.92

Table 13 Forecast data of wind renewable energy consumption in the USA from 2020 to 2024

Year	2020	2021	2022	2023	2024
Consumption	2891.57	3087.41	3283.29	3479.21	3675.16

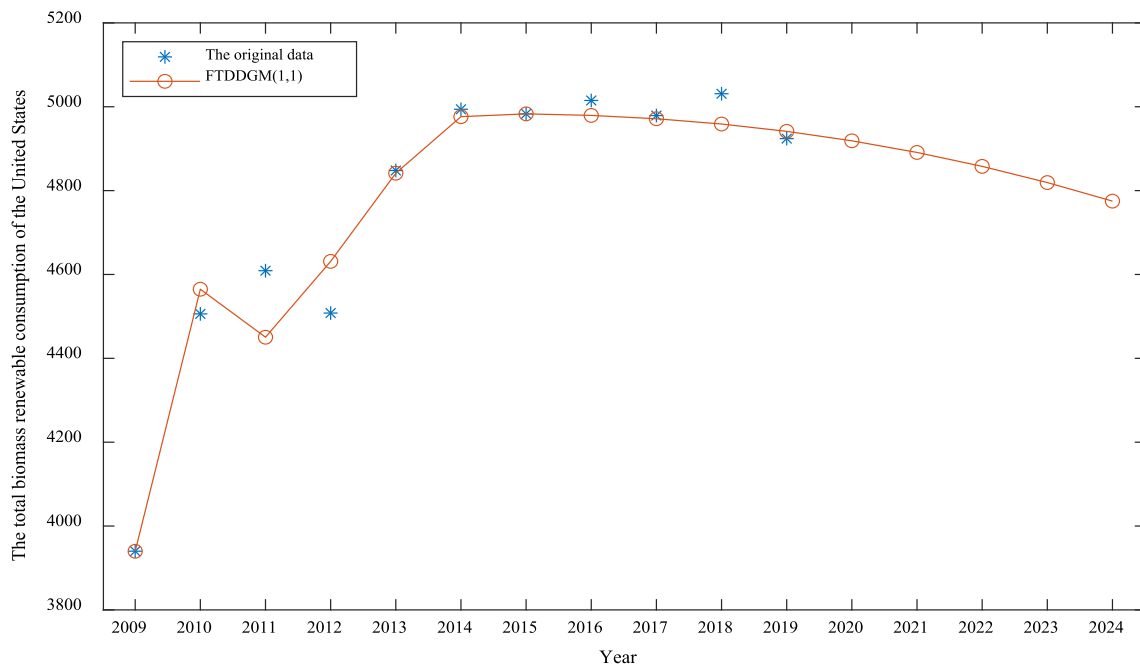


Fig. 14 Prediction trend of FTDDGM(1,1) with variable weight buffer in Case 2

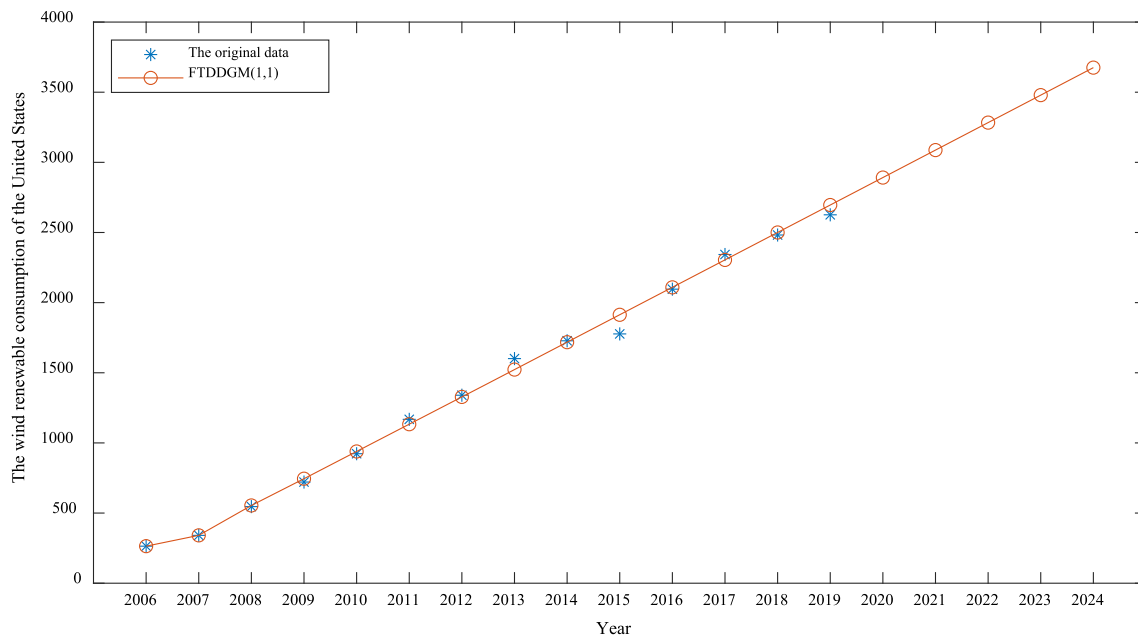


Fig. 15 Prediction trend of FTDDGM(1,1) with variable weight buffer in Case 3

consumption data from 2009 to 2015 will be used as the training set to establish FTDDGM(1,1) model with variable weight buffer operator. The forecast results of solar renewable energy consumption in the USA from 2020 to 2024 are recorded in Table 11, and the prediction trend is shown in Fig. 13.

According to the forecast results in Table 11 and Fig. 13, the solar renewable energy consumption in the USA will keep increasing year by year from 2020 to 2024. As the USA solar power industry has received strong support from government funds and policies, a large number of solar power generation facilities have been put into use, increasing the proportion of solar renewable energy consumption in energy consumption. Therefore, the forecast results of this case conforms to the objective reality.

Case 2 Forecast of total biomass renewable energy consumption of the USA from 2020 to 2024.

In Case 2 of Sect. 4.2, the FTDDGM(1,1) model with variable weight buffer operator was established by using the total biomass renewable energy consumption data in the USA from 2009 to 2015, and the MAPEp value of the data from 2016 to 2019 was only 0.66274, so this case continues to use the USA total biomass renewable energy consumption data from 2009 to 2015 as the training set to establish the FTDDGM(1,1) model with variable weight buffer operator. Forecast the total biomass renewable energy consumption in the USA from 2020 to 2024. The forecast results are recorded in Table 12, and the prediction trend is shown in Fig. 14.

According to the forecast results in Table 12 and Fig. 14, the total biomass renewable energy consumption in the USA will decrease year by year from 2020 to 2024. As a renewable fuel, the total biomass energy is mainly used in industry and transportation, due to the COVID-19 pandemic, the use of transportation and transportation industries in the USA declined. Therefore, the forecast results of this case conforms to the objective reality.

Case 3 Forecast of wind renewable energy consumption of the USA from 2020 to 2024.

In this case, the US wind renewable energy consumption data from 2009 to 2015 is used as the training set, and the FTDDGM(1,1) model with variable weight buffer operator is established. The forecast results for the US wind renewable energy consumption from 2020 to 2024 are recorded in Table 13 and the prediction trend is shown in Fig. 15.

According to the forecast results in Table 13 and Fig. 15, the wind renewable energy consumption will keep increasing year by year from 2020 to 2024. As the wind power industry in the USA has attracted a large amount of investment, as well as the encouragement of the finance and policies, the wind power industry has developed rapidly, and the wind renewable energy consumption has also maintained a steady increase. Therefore, the forecast results of this case conforms to the objective reality.

5 Conclusion

In this paper, a novel fractional time delay discrete model is proposed by introducing the fractional time delay term and combining with the discrete modeling technology, and the parameter estimation and time response formula of the new model are deduced. In order to improve the prediction accuracy of the new model, the variable weight buffer operator is introduced, and it is proved that the combination of the new model and the variable weight buffer operator satisfies the new information first principle of the last modeling data. The FTDDGM(1,1) model is simple in structure and easy to analyse its properties. The variable weight buffer operator enhances the importance of new information in disguise by adding up the elements in the sequence with the latest elements in a certain proportion. In Case 2, other grey models focus too much on the overall information and ignore the trend of new information change, which leads to unsatisfactory final prediction results. The fractional order operator can fine tune the parameters of the model and the FTDDGM(1,1) model observes the trend of new element change, so the FTDDGM(1,1) model has better prediction results and adaptability than other grey models through the analysis of three actual cases of solar energy, wind energy consumption and biomass consumption.

In order to verify the practicability of FTDDGM(1,1) with variable weight buffer operator in the renewable energy case of the United States. Build a prediction model for the USA solar energy, total biomass energy and wind energy datasets. According to the experimental results, the MAPEs and MAPE_p values of FTDDGM(1,1) with variable weight buffer operator are smaller than the other five models, showing better simulation and prediction accuracy than the other five models. At the same time, the values of each model are compared and analysed, and the value of FTDDGM(1,1) with variable weight buffer operator has the lowest variation range, showing better stability than the other five models. Therefore, the FTDDGM(1,1) with variable weight buffer operator is used to predict the solar energy, total biomass energy, and wind energy consumption in the USA from 2020 to 2024.

According to the prediction results in Sect. 4.3, the consumption of solar energy and wind energy in the USA will show an increasing trend in the future. The growth rate of solar energy and wind energy consumption will increase in 2020 and decrease year by year from 2021 to 2024. In view of this phenomenon, the government should increase financial and policy support for solar and wind energy, promote the development of solar and wind energy industries, and advocate the use of solar and wind energy to promote the development of renewable energy, so as to

optimize the energy structure. The total biomass consumption showed a trend of gradual decline, lead to this phenomenon may be COVID—19 during a pandemic, the US department of transportation of the biomass energy consumption decreased, so the government need to guarantee the development of biomass energy at the same time, increasing the rest of the clean energy investment, so as to ensure the renewable energy in the energy structure will occupy the important position in the future.

In today's global energy structure optimization trend, the development of renewable energy is conducive to economic, environmental and energy development. Therefore, FTDDGM(1,1) with variable weight buffer operator is constructed in this paper to reasonably forecast the consumption of renewable energy in the USA, providing reference for policymaking, government expenditure arrangement and project planning. Meanwhile, FTDDGM(1,1) with variable weight buffer operator can be applied to other fields.

Author contributions All authors, Yong Wang, Pei Chi, Rui Nie, Xin Ma, Wenqing Wu and Binghong Guo, wrote the paper jointly and contributed equally to this work. All authors read and approved the final manuscript.

Funding This work was supported by the Natural Science Foundation of Sichuan Province (No. 2023NSFSC0428).

Data availability Enquiries about data availability should be directed to the authors.

Declarations

Conflict of interest The authors declare that they have no known competing financial interests or personal relationships that could have appeared to influence the work reported in this paper.

Ethical approval This article does not contain any studies with human participants or animals performed by any of the authors.

References

- Brodny J, Tutak M, Saki SA (2020) Forecasting the structure of energy production from renewable energy sources and biofuels in Poland. *Energies* 13(10):2539
- Dai XZ, Zhang Z, Wang Y, Li JZ, Chen L (2014) Multi-parameter magnetoelectric response modeling of magnetostrictive/piezoelectric laminate composites considering shear strain. *J Appl Phys* 115(1):014104
- Deng JL (1982) Control problems of grey systems. *Syst Control Lett* 1(5):288–294
- Feng ZH, Wang Y, Ma X (2020) Asymptotically almost periodic solutions for certain differential equations with piecewise constant arguments. *Adv Differ Equ* 2020(1):242
- He XB, Wang Y, Zhang YY, Ma X, Wu WQ, Zhang L (2022) A novel structure adaptive new information priority discrete grey

- prediction model and its application in renewable energy generation forecasting. *Appl Energy* 325:119854
- Huang YS, Yang L, Gao C, Jiang YQ, Dong YL (2020) A novel prediction approach for short-term renewable energy consumption in china based on improved Gaussian process regression. *Energies* 12(21):4181
- Khan PW, Byun YC, Lee SJ, Kang DH, Kang JY, Park HS (2020) Machine learning-based approach to predict energy consumption of renewable and nonrenewable power sources. *Energies* 13(18):4870
- Khan ZA, Hussain T, Baik SW (2022) Boosting energy harvesting via deep learning-based renewable power generation prediction. *J King Saud Univ Sci* 34(3):101815
- Kilic F (2022) Forecasting the electricity capacity and electricity generation values of wind & solar energy with artificial neural networks approach: the case of Germany, applied artificial intelligence. *J King Saud Univ Sci*. <https://doi.org/10.1080/08839514.2022.2033911>
- Liu LY, Wu LF (2020) Forecasting the renewable energy consumption of the European countries by an adjacent non-homogeneous grey model. *Appl Math Model* 89:1932–1948
- Ma J, Opong A, Acheampong KN, Aburuquah LA (2018) Forecasting renewable energy consumption under zero assumptions. *Sustainability* 10(3):576
- Ma X, Liu ZB, Wang Y (2019a) Application of a novel nonlinear multivariate grey Bernoulli model to predict the tourist income of China. *J Comput Appl Math* 347:84–94
- Ma X, Wu W, Zhang Y (2019b) Improved GM(1,1) model based on Simpson formula and its applications. *J Grey Syst* 31(4):33–46
- Ma X, Xie M, Wu WQ, Zeng B, Wang Y, Wu XX (2019c) The novel fractional discrete multivariate grey system model and its applications. *Appl Math Model* 70:402–424
- Ma X, Mei X, Wu WQ, Wu XX, Zeng B (2019d) A novel fractional time delayed grey model with Grey Wolf Optimizer and its applications in forecasting the natural gas and coal consumption in Chongqing China. *Energy* 178:487–507
- Ma X, Wu WQ, Zeng B, Wang Y, Wu XX (2020) The conformable fractional grey system model. *ISA Trans* 96:255–271
- Mao SH, Gao MY, Xiao XP, Zhu M (2016) A novel fractional grey system model and its application. *Appl Math Model* 40:5063–5076
- Mehedintu A, Sterpu M, Soava G (2018) Estimation and forecasts for the share of renewable energy consumption in final energy consumption by 2020 in the European Union. *Sustainability* 10(5):1515
- Meng W, Li Q, Zeng B, Yang YJ (2020) FDGM(1,1) model based on unified fractional grey generation operator. *Grey Syst Theory Appl*. <https://doi.org/10.1108/GS-07-2020-0093>
- Mirjalili S (2015) How effective is the Grey Wolf Optimizer in training multi-layer perceptrons. *Appl Intell* 43(1):150–161
- Mirjalili S, Mirjalili SM, Lewis A (2014) Grey wolf optimizer. *Adv Eng Softw* 69:46–61
- Rehbein JA, Watson JEM, Lane JL, Sonter LJ, Venter O, Atkinson SC, Allan JR (2020) Renewable energy development threatens many globally important biodiversity areas. *Glob Change Biol* 26(5):3040–3051
- Sharif A, Mishra S, Sinha A, Jiao ZL, Shahbaz M, Afshan S (2020) The renewable energy consumption-environmental degradation nexus in Top-10 polluted countries: fresh insights from quantile-on-quantile regression approach. *Renew Energy* 150:67–690
- Swewart GM (1977) On the perturbation of pseudoinverses, projections and linear square problem. *SIAM Rev* 19:634–662
- U.S. Energy Information Administration, <https://www.eia.gov/totalenergy/data/browser/?tbl=T10.01#/>
- Wang Y, Yi XY (2017) Transient pressure behavior of a fractured vertical well with a finite-conductivity fracture in triple media carbonate reservoir. *J Porous Media* 20(8):707–722
- Wang Y, Yi XY (2018) Flow modeling of well test analysis for a multiple-fractured horizontal well in triple media carbonate reservoir. *Int J Nonlinear Sci Numer Simul* 19(5):439–457
- Wang ZX, Dang YG, Liu SF (2009) Buffer operators with variable weights and the complement of axioms. *Syst Eng* 27(1):113–117 (in Chinese)
- Wang Y, Tao ZW, Chen L, Ma X (2017) The nonlinear oil-water two-phase flow behavior for a horizontal well in triple media carbonate reservoir. *Acta Geophys* 65(5):977–989
- Wang Y, Li MJ, Ma X, Gao WB, Xue GQ, Zhou J (2018a) Modeling the nonlinear oil-water two-phase flow behavior for a multiple-fractured horizontal well in triple media carbonate reservoir. *Adv Appl Math Mech* 10(4):998–1024
- Wang Y, Zhang C, Huang R, Cao HT, Ma X (2018b) Modeling oil-water two-phase flow behavior of a fractured vertical well with a finite-conductivity fracture in triple media carbonate reservoir. *Adv Appl Math Mech* 10(3):581–610
- Wang Y, Zhang C, Chen T, Ma X (2018c) Modeling the nonlinear flow for a multiple-fractured horizontal well with multiple finite-conductivity fractures in triple media carbonate reservoir. *J Porous Media* 21(12):1283–1305
- Wang Y, Tian DH, Li GF, Zhang C, Chen T (2019) Dynamic analysis of a fractured vertical well in a triple media carbonate reservoir. *Chem Technol Fuels Oils* 55(1):56–65
- Wang Y, Tao ZW, Tian DH, Ma X, Feng ZH (2020a) Optimizing injection process of water-alternate-gas using different produced gas densities in enriched-gas flooding. *Chem Technol Fuels Oils* 56(2):271–284
- Wang Y, Tao ZW, Feng ZH (2020b) Dynamic analysis of oil-water two-phase flow for a multiple-fractured horizontal well with multiple finite-conductivity fractures in triple media carbonate reservoir. *ZAMM-Zeitschrift Fur Angewandte Mathematik Und Mechanik* 100(4):e201900046
- Wang Y, Tao ZW, Tian DH, Ma X, Li MJ, Feng ZH (2020c) Some novel results of T-periodic solutions for Rayleigh type equation with double deviating arguments. *Univ Politehnica Bucharest Sci Bull Ser A-Appl Math Phys* 82(1):55–68
- Wang Y, Nie R, Ma X, Liu ZB, Chi P, Wu WQ, Guo BH, Yang XP, Zhang LF (2021) A novel Hausdorff fractional NGMC(p, n) grey prediction model with Grey Wolf Optimizer and its applications in forecasting energy production and conversion of China. *Appl Math Model* 97:381–397
- Wang M, Wang W, Wu LF (2022a) Application of a new grey multivariate forecasting model in the forecasting of energy consumption in 7 regions of China. *Energy* 243:123024
- Wang Y, Wang L, Ye LL, Ma X, Wu WQ, Yang ZS, He XB, Zhang L, Zhang YY, Zhou Y, Luo YX (2022b) A novel self-adaptive fractional multivariable grey model and its application in forecasting energy production and conversion of China. *Eng Appl Artif Intell* 115:105319
- Wang Y, Nie R, Chi P, Ma X, Wu WQ, Guo BH, He XB, Zhang L, Zhang YY (2022c) A novel fractional structural adaptive grey Chebyshev polynomial Bernoulli model and its application in forecasting renewable energy production of China. *Expert Syst Appl* 210:118500
- Wang Y, Ye LL, Yang ZS, Ma X, Wu WQ, Wang L, He XB, Zhang L, Zhang YY, Zhou Y, Luo YX (2022d) A novel structure adaptive fractional discrete grey forecasting model and its application in China's crude oil production prediction. *Expert Syst Appl* 207:118104
- Wang Y, Yang ZS, Wang L, Ma X, Wu WQ, Ye LL, Zhou Y, Luo YX (2022e) Forecasting China's energy production and

- consumption based on a novel structural adaptive Caputo fractional grey prediction model. *Energy* 259:124935
- Wang Y, He XB, Zhang L, Ma X, Wu WQ, Nie R, Chi P, Zhang YY (2022f) A novel fractional time-delayed grey Bernoulli forecasting model and its application for the energy production and consumption prediction. *Eng Appl Artif Intell* 110:104683
- Wang Y, Chi P, Nie R, Ma X, Wu WQ, Guo BH (2022g) Self-adaptive discrete grey model based on a novel fractional order reverse accumulation sequence and its application in forecasting clean energy power generation in China. *Energy* 253:124093
- Wang Y, Zhang L, He XB, Ma X, Wu WQ, Nie R, Chi P, Zhang YY (2023a) A novel exponential time delayed fractional grey model and its application in forecasting oil production and consumption of China. *Cybern Syst* 54(2):168–196
- Wang Y, Yang ZS, Ye LL, Wang L, Zhou Y, Luo YX (2023b) A novel self-adaptive fractional grey Euler model with dynamic accumulation order and its application in energy production prediction of China. *Energy* 265:126384
- Wu LF, Liu SF, Yao LG, Yan SL, Liu DL (2013) Grey system model with the fractional order accumulation. *Commun Nonlinear Sci Numer Simul* 18:1775–1785
- Wu LF, Liu SF, Yang YJ, Ma LH, Liu HX (2016) Multi-variable weakening buffer operator and its application. *Inf Sci* 339:98–107
- Wu LF, Gao X, Xiao Y, Yang Y, Chen X (2018a) Using a novel multi-variable grey model to forecast the electricity consumption of Shandong province in china. *Energy* 157:327–335
- Wu WQ, Ma X, Zeng B, Wang Y, Cai W (2018b) Application of the novel fractional grey model FAGMO(1,1, k) to predict China's nuclear energy consumption. *Energy* 165:223–234
- Wu WQ, Ma X, Zeng B, Wang Y, Cai W (2019a) Forecasting short-term renewable energy consumption of China using a novel fractional nonlinear grey Bernoulli model. *Renew Energy* 140:70–87
- Wu WQ, Ma X, Zhang YY, Wang Y, Wu XX (2019b) Analysis of novel FAGM(1,1, t) model to forecast health expenditure of China. *Grey Syst Theory Appl* 9(2):232–250
- Wu WQ, Ma X, Wang Y, Zhang YY, Zeng B (2019c) Research on a novel fractional GM(alpha, n) model and its applications. *Grey Syst Theory Appl* 9(3):356–373
- Wu WQ, Ma X, Zhang YY, Li WP, Wang Y (2020a) A novel conformable fractional non-homogeneous grey model for forecasting carbon dioxide emissions of BRICS countries. *Sci Total Environ* 707:135447
- Wu WQ, Ma X, Wang Y, Cai W, Zeng B (2020b) Predicting China's energy consumption using a novel grey Riccati model. *Appl Soft Comput* 95:106555
- Wu WQ, Ma X, Zeng B, Lv WY, Wang Y, Li WP (2020c) A novel Grey Bernoulli model for short-term natural gas consumption forecasting. *Appl Soft Comput* 84:393–404
- Wu W, Ma X, Wang Y, Cai W, Zeng B (2021) Predicting primary energy consumption using NDGM(1,1, k, c) model with Simpson formula. *Sci Iran* 28(6):3379–3395
- Xie NM, Liu SF (2003) A new applicative weakening buffer operator. *Chin J Polym Sci* 11:46–48
- Xie NM, Liu SF (2009) Discrete grey forecasting model and its optimization. *Appl Math Model* 33:1173–1186
- Yamaguchi D, Li GD, Naga M (2007) A grey-based rough approximation model for interval data processing. *Inf Sci* 177:4727–4744
- Yan Q, Dai XZ, Zhang Z, Wang LJ, Wang Y (2022) Broadband vibration energy harvester based on nonlinear magnetic force and rotary pendulums. *Smart Mater Struct* 31(1):015035
- Yao LJ, Feng ZH, Wang Y (2022) A representation of bifinite domains by rough approximable concepts. *J Intell Fuzzy Syst* 43(5):5703–5708
- Yu L, Ma X, Wu WQ, Xiang XW, Wang Y, Zeng B (2021a) application of a novel time-delayed power-driven grey model to forecast photovoltaic power generation in the Asia-Pacific region. *Sustain Energy Technol Assess* 44:100968
- Yu L, Ma X, Wu WQ, Wang Y, Zeng B (2021b) A novel elastic net-based NGBMC(1, n) model with multi-objective optimization for nonlinear time series forecasting. *Commun Nonlinear Sci Numer Simul* 96:105696
- Zeng B, Ma X, Zhou M (2020a) A new-structure grey Verhulst model for China's tight gas production forecasting. *Appl Soft Comput* 96:106600
- Zeng B, Li H, Ma X (2020b) A novel multi-variable grey forecasting model and its application in forecasting the grain production in China. *Comput Ind Eng* 150:106915
- Zeng B, Zhou M, Liu XZ, Zhang ZW (2020c) Application of a new grey prediction model and grey average weakening buffer operator to forecast China's shale gas output. *Energy Rep* 6:1608–1618
- Zeng B, Tong MY, Ma X (2020d) A new-structure grey Verhulst model: development and performance comparison. *Appl Math Model* 82:522–537
- Zhang K, Qu P, Zhang Y (2015) Delay multi-variables discrete grey model and its application. *Syst Eng Theory Pract* 35(8):2092–2013
- Zhou XY, Gao YQ, Yao WX, Yu NP (2022) A robust segmented mixed effect regression model for baseline electricity consumption forecasting. *J Mod Power Syst Clean Energy* 10(1):71–80

Publisher's Note Springer Nature remains neutral with regard to jurisdictional claims in published maps and institutional affiliations.

Springer Nature or its licensor (e.g. a society or other partner) holds exclusive rights to this article under a publishing agreement with the author(s) or other rightsholder(s); author self-archiving of the accepted manuscript version of this article is solely governed by the terms of such publishing agreement and applicable law.